OXFORD

molecular human reproduction

Molecular Human Reproduction, 2023, **29(9)**, gaad029

https://doi.org/10.1093/molehr/gaad029
Advance Access Publication Date: August 23, 2023
Original Research

TRPV2, a novel player in the human ovary and human granulosa cells

Katja Eubler[1], Karolina M. Caban[2], Gregory A. Dissen[3], Ulrike Berg[4], Dieter Berg[4], Carola Herrmann[1], Nicole Kreitmair[1], Astrid Tiefenbacher[1], Thomas Fröhlich [2], and Artur Mayerhofer [1,*]

[1]Biomedical Center Munich (BMC), Cell Biology, Anatomy III, Faculty of Medicine, Ludwig-Maximilian-University (LMU) Munich, Planegg-Martinsried, Germany
[2]Laboratory for Functional Genome Analysis LAFUGA, Gene Center, LMU Munich, Munich, Germany
[3]Molecular Virology Core, Oregon Health & Science University (OHSU), Oregon National Primate Research Center, Beaverton, OR, USA
[4]A.R.T. Bogenhausen, Munich, Germany

*Correspondence address. Biomedical Center Munich (BMC), Cell Biology, Anatomy III, Faculty of Medicine, Ludwig-Maximilian-University (LMU) Munich, Großhaderner Strasse 9, 82152 Planegg-Martinsried, Germany. E-mail: mayerhofer@bmc.med.lmu.de https://orcid.org/0000-0002-9388-4639

Abstract

The cation channel 'transient receptor potential vanilloid 2' (TRPV2) is activated by a broad spectrum of stimuli, including mechanical stretch, endogenous and exogenous chemical compounds, hormones, growth factors, reactive oxygen species, and cannabinoids. TRPV2 is known to be involved in inflammatory and immunological processes, which are also of relevance in the ovary. Yet, neither the presence nor possible roles of TRPV2 in the ovary have been investigated. Data mining indicated expression, for example, in granulosa cells (GCs) of the human ovary *in situ*, which was retained in cultured GCs derived from patients undergoing medical reproductive procedures. We performed immunohistochemistry of human and rhesus monkey ovarian sections and then cellular studies in cultured GCs, employing the preferential TRPV2 agonist cannabidiol (CBD). Immunohistochemistry showed TRPV2 staining in GCs of large antral follicles and corpus luteum but also in theca, endothelial, and stromal cells. TRPV2 transcript and protein levels increased upon administration of hCG or forskolin. Acutely, application of the agonist CBD elicited transient Ca^{2+} fluxes, which was followed by the production and secretion of several inflammatory factors, especially COX2, IL6, IL8, and PTX3, in a time- and dose-dependent manner. CBD interfered with progesterone synthesis and altered both the proteome and secretome, as revealed by a proteomic study. While studies are somewhat hampered by the lack of highly specific TRPV2 agonist or antagonists, the results pinpoint TRPV2 as a modulator of inflammation with possible roles in human ovarian (patho-)physiology. Finally, as TRPV2 is activated by cannabinoids, their possible ovarian actions should be further evaluated.

Keywords: ion channel / calcium / female gonad / follicle / corpus luteum / inflammation / cannabidiol

Introduction

Transient receptor potential vanilloid 2, TRPV2, is regarded as one of the least-characterized members of the TRP-family of ion channels (Perálvarez-Marín *et al.*, 2013). This non-selective cation channel is mostly permeable to Ca^{2+} ions and can be activated by heat, red light, mechanical stretch, reactive oxygen species (ROS), hormones and growth factors, chemical compounds, and also cannabinoids (Caterina *et al.*, 1999; Kanzaki *et al.*, 1999; Neeper *et al.*, 2007; Qin *et al.*, 2008; Monet *et al.*, 2009; Shibasaki *et al.*, 2010; Zhang *et al.*, 2012; Kojima and Nagasawa, 2014; Shibasaki, 2016; Oda *et al.*, 2021).

With regard to function, TRPV2 has been linked to inflammatory and immunological processes as it is highly expressed in macrophages, mast cells, and adaptive immune cells (Nagasawa *et al.*, 2007; Link *et al.*, 2010; Yamashiro *et al.*, 2010; Santoni *et al.*, 2013). It has, however, also been linked to cancer invasiveness and progression and was proposed as a biomarker and potential therapeutic target (Monet *et al.*, 2010; Elbaz *et al.*, 2018; Santoni *et al.*, 2020; Siveen *et al.*, 2020; Kato *et al.*, 2022).

Little is known about TRPV2 and the cells of the gonads, in general. Yet, this ion channel was demonstrated to be highly abundant in several cells of the human testis, including testicular macrophages and peritubular (myoid) cells (Eubler *et al.*, 2018, 2021). Results obtained by these studies suggested that TRPV2 is a new player within the testicular channelome and is involved in inflammatory processes and hence fertility/infertility.

Regarding the human ovary, a search in available published data indicated that TRPV2 is present in the female gonad *in situ*, specifically in human granulosa cells (GCs), endothelial cells, smooth muscle cells, and macrophages (Human Protein Atlas—https://www.proteinatlas.org/ENSG00000187688-TRPV2/single+cell+type/ovary; accessed on 15 March 2023) and in IVF-derived cultured human GCs (Bagnjuk *et al.*, 2019; Beschta *et al.*, 2021; Supplementary Fig. S1A). Further data mining revealed that *TRPV2* transcript levels increased in human GCs in parallel with follicle development (Zhang *et al.*, 2018; Supplementary Fig. S1B) and in the late to very late stages of the rhesus monkey corpus luteum (Bogan *et al.*, 2008; Supplementary Fig. S1C). Mechanical forces and ROS are activators of TRPV2 and play roles in the human ovary, especially in follicles and/or the corpus luteum (Matousek *et al.*, 2001; Prasad *et al.*, 2016; Buck *et al.*, 2019; Sun *et al.*, 2021). For instance, in preovulatory follicles, where mechanical stress is high and where ROS are produced

Received: April 03, 2023. **Revised:** June 29, 2023. **Editorial decision:** August 21, 2023.

(Matousek et al., 2001; Buck et al., 2019), there is an inflammatory milieu with high cytokine levels, of interleukin (IL) 6 and 8 among others, which is thought to be essential for ovulation. Human GCs are known producers of such proinflammatory molecules (Machelon et al., 1994; Runesson et al., 1996; Duffy et al., 2019; Piccinni et al., 2021) and increased levels are reported in polycystic ovarian syndrome (PCOS; Adams et al., 2016), the most common endocrine disorder of reproductive-aged women, which is associated with systemic low-grade inflammation.

The paucity of information on TRPV2 and its roles in the ovary and the results of data mining led us to initiate a series of studies. We reasoned that studies of human GCs, derived from preovulatory follicles of IVF patients and transferred to *in vitro* cell culture conditions, may be instructive. We examined the regulation and functionality of TRPV2 and studied the consequences of its activation. We employed a pharmacological activator, cannabidiol (CBD), which has been identified as a preferential activator of TRPV2 (Qin et al., 2008; De Petrocellis et al., 2011; Pumroy et al., 2019; Landucci et al., 2022), and examined Ca^{2+} conductivity as well as cytokine and progesterone secretion and performed a proteomic analysis.

Materials and methods

Isolation and culture of human GCs

Human GCs were isolated from follicular fluids derived from patients undergoing standard IVF or oocyte cryopreservation. The scientific use of the obtained biological material was approved by the Ethics Committee of Ludwig-Maximilian-University Munich (Project number 20-697). The patients consented in written to the use of the cells, as part of an ongoing German Research Foundation (DFG)-funded project (MA 1080/31-1; project number 456828204).

For cell isolation, the follicular fluids of 2–8 anonymized patients were pooled and strained using 40-µm mesh size cell strainers (Greiner Bio-One, Frickenhausen, Germany). Cells were extracted from the strainer and transferred to pure Dulbecco's modified Eagle medium/Ham's F-12 nutrient mixture (DMEM/F-12; Gibco, Paisley, UK). The suspension was centrifuged at 800–1000 rpm (equivalent to ~230*g*) for 3 min, resuspended in DMEM/F-12 supplemented with 10% fetal calf serum (FCS; Capricorn Scientific, Ebsdorfergrund, Germany) and 1% penicillin/streptomycin (P/S; BioChrom, Berlin, Germany). The cell number was determined by staining the cells with trypan blue (Lonza, Basel, Switzerland) and by using a Neubauer chamber. A total of 1–1.5 × 10^5 cells was seeded onto 35 mm tissue culture dishes (Sarstedt, Nümbrecht, Germany) and kept at 37°C, 5% CO_2, and 95% humidity until experimental use. To get rid of the remaining tissue fragments and blood cells, the meanwhile adherent GCs were washed thoroughly with pure DMEM/F-12 and fresh medium supplemented with FCS and P/S was added. Cell culture conditions did not exceed 7 days; the medium was changed regularly and human GCs were thoroughly washed with phosphate-buffered saline (PBS; Thermo Fisher Scientific, Waltham, WA, USA) prior to any further processing.

RNA isolation and quantitative RT-PCR

The RNeasy Plus Micro Kit (Qiagen, Hilden, Germany) was utilized to isolate RNA, following the manufacturer's instructions. Depending on the RNA amount, 200–1000 ng were subjected to reverse transcription using SuperScript™ II (Invitrogen, Carlsbad, CA, USA), followed by quantitative RT-PCR (QuantiFast SYBR Green PCR Kit, Qiagen, Hilden, Germany; LightCycler 96® System, Roche Diagnostics, Penzberg, Germany) with 4 ng cDNA within the reaction. The housekeeping genes Peptidylprolyl isomerase A (*PPIA*) and ribosomal protein L19 (*L19*) served as internal controls; the geometric mean of their mRNA levels was used for normalization. Changes in gene expression were analyzed according to the $2^{-\Delta\Delta Cq}$ method, as described before (Pfaffl, 2001). Detailed information on the utilized oligonucleotide primers is provided in Table 1.

Protein isolation and western blots

Human GCs were lysed with radioimmunoprecipitation assay buffer supplemented with protease and phosphatase inhibitors (Thermo Fisher Scientific). The resulting suspension was sonicated and centrifuged at 13 000 rpm (equivalent to ~16 000*g*) at 4°C for 15 min. Protein concentrations were determined by Lowry assay (DCTM Protein Assay; Bio-Rad Laboratories, Hercules, CA, USA), and equal amounts of protein (6–10 µg/lane) were loaded. Nitrocellulose membranes (Macherey-Nagel, Düren, Germany) were incubated either with a polyclonal TRPV2 antibody raised in rabbit (HPA044993; Atlas Antibodies, Stockholm, Sweden) or a monoclonal TRPV1 antibody raised in mouse (66983-1-Ig; Proteintech, Planegg-Martinsried, Germany) overnight at 4°C, followed by incubation with a monoclonal β-actin antibody raised in mouse (A5441, Sigma-Aldrich, St. Louis, MI, USA) for 1 h at room temperature. Adequate IRDye® secondary antibodies were used (800CW donkey-α-rabbit, 926-32213; 680RD donkey-α-mouse, 926-68072; Li-COR Biosciences, Lincoln, NE, USA) and bands were detected using the Odyssey CLx imaging system (Li-COR Biosciences).

Immunohistochemistry and immunocytochemistry

Tissue sections of human and rhesus ovaries were subjected to immunohistochemistry (IHC). They were cut from paraffin-embedded blocks, which were used in previous studies (Blohberger et al., 2015; Buck et al., 2019). In brief, the paraffin samples stem from adult rhesus monkey ovaries (n = 4), provided by the Oregon National Primate Research Center (ONPRC) at Oregon Health and Science University (OHSU; Beaverton, OR, USA). The animal husbandry and use were performed according to, and approved by, the institutional animal care and use committee (IACUC) of the ONPRC/OHSU. IHC was performed using archival human ovarian sections as described (Blohberger et al., 2015). Cultured human GCs from culture Day 3 were used for immunocytochemical (ICC) staining, as described previously (Buck et al., 2019). The same primary antibody against TRPV2 used for Western Blot was used for IHC and ICC. For IHC, TRPV2-binding sites were visualized using a biotinylated α-rabbit secondary antibody (111-065-144; Jackson Immunoresearch Labs, West Grove, PA, USA), an avidin-biotin complex peroxidase (Vector Laboratories), and DAB (Sigma-Aldrich) and sections were slightly counterstained with hematoxylin. For ICC, TRPV2-binding sites were visualized with a fluorescence conjugated α-rabbit secondary antibody (Cy5 donkey-α-rabbit, 711-175-152; Dianova, Hamburg, Germany) and DNA was stained using DAPI. Omission of primary antibody, rabbit IgG controls, and pre-adsorption with the respective peptides (APrEST83822, Atlas Antibodies, Stockholm, Sweden) served as negative controls.

Reagents and treatment of human GCs

To monitor the expression of TRPV2 over culture time, mRNA and protein from untreated young (Days 1–2), intermediate (Days 3–4), and old (Days 5–6 for transcript; Days 5–7 for protein)

Table 1. List of oligonucleotide primer sequences.

Gene name	Reference ID	Nucleotide sequence	Amplicon size (bp)
L19	NM_000981.3	5′-AGG CAC ATG GGC ATA GGT AA-3′ 5′-CCA TGA GAA TCC GCT TGT TT-3′	199
PPIA	NM_021130.4	5′-AGA CAA GGT CCC AAA GAC-3′ 5′-ACC ACC CTG ACA CAT AAA-3′	118
CD147	NM_001728.4	5′-TGG AAG GCA ATC CTG AAA TC-3′ 5′-CTC CGA CCA GGC CAT CAT C-3′	234
COX2	NM_000963.3	5′-CTT ACC CAC TTC AAG GGA-3′ 5′-GCC ATA GTC AGC ATT GTA AG-3	132
CXCL1	NM_001511.3	5′-CGC CCA AAC CGA AGT CAT AG-3′ 5′-CTC TGC AGC TGT GTC TCT CT-3′	211
CYP19A1	NM_000103	5′-GCT ACC CAG TGA AAA AGG GGA-3′ 5′-GCC AAA TGG CTG AAA GTA CCT AT-3′	140
DPP4	NM_001935.3	5′-GGC TGG TCA TAT GGA GGG TA-3′ 5′-CAG GGC TTT GGA GAT CTG AG-3′	273
IL6	NM_000600.4	5′-AAC CTG AAC CTT CCA AAG ATG G-3′ 5′-TCT GGC TTG TTC CTC ACT ACT-3′	159
IL8	NM_000584.3	5′-TCT TGG CAG CCT TCC TGA-3′ 5′-GAA TTC TCA GCC CTC TTC-3′	190
MCP1	NM_002982.3	5′-AGG TGA CTG GGG CAT TGA T-3′ 5′-GAA GTG ATG GGT ATC CGG TC-3′	109
OPN	NM_001040058.1	5′-TTT TCA CTC CAG TTG TCC CC-3′ 5′-TAC TGG ATG TCA GGT CTG CG-3′	109
P450scc	NM_001099773	5′-TCG GCA GCC TGG AAG AAA GAC C-3′ 5′-GGC GCT CCC CAA AAA TGA CG-3′	226
PTX3	NM_002852.3	5′-TAG TGT TTG TGG TGG GTG GA-3′ 5′-TGT GAG CCC TTC CTC TGA AT-3′	110
StAR	NM_000349	5′-ACG TGG ATT AAC CAG GTT CG-3′ 5′-CAG CCC TCT TGG TTG CTA AG-3′	149
THBS1	NM_003246.3	5′-AGT CGT CTC TGC AAC AAC CC-3′ 5′-AGC TAG TAC ACT TCA CGC CG-3′	148
TRPV2	NM_016113.4	5′-CCA GCA AGT ACC TCA CCG AC-3′ 5′-CAG GCA TTG ACT CCG TCC TT-3′	100

cultured human GCs were extracted and subjected to quantitative RT-PCR or western blot, respectively. Any pharmacological treatment was carried out using human GCs from cell culture Day 3 and to synchronize cell cycle and metabolism; cells were starved for 2 h on DMEM/F-12 with 1% P/S but reduced FCS content (2%) prior to any application. Potential hormonal regulation of TRPV2 expression was evaluated by the treatment of human GCs for 24 h with 10 IU/ml human chorionic gonadotropin (hCG) (Sigma-Aldrich), or with an equal volume of the corresponding solvent control PBS (Thermo Fisher Scientific), respectively. A possible cAMP-dependent regulation was investigated using 50 µM forskolin (FSK; Sigma-Aldrich) or, as a control, an equal volume of the solvent, ethanol (EtOH) for 24 h. TRPV2 channel functionality was examined by incubation of human GCs with 1, 6, 10, or 30 µM of the known activator CBD (Tocris Bioscience, Bristol, UK) or, as a control, an equal volume of the solvent EtOH (Qin *et al.*, 2008). To circumvent any interference with cannabinoid receptors (CNR1 and CNR2), specific blockers, i.e. AM251 (80 nM; Tocris Bioscience) and AM630 (800 nM; Tocris Bioscience), were added 1 h in advance to CBD application, as described in earlier studies (Eubler *et al.*, 2018, 2021). Application of the blockers served as a control and neither their presence nor administration of equal volumes of the corresponding solvents (EtOH and dimethylsulfoxide) resulted in any significant changes in transcript levels of *TRPV2*, *IL6*, *IL8*, or *PTX3* compared to untreated cultured human GCs (Supplementary Fig. S2).

Ca^{2+} imaging

Acute channel activation was examined by means of Ca^{2+} imaging. For the experiments, 5–7 × 10^4 human GCs were seeded on imaging µ-dishes (µ-Dish$^{35\,mm,low}$ with polymer coverslip; ibidi, Gräfelfing, Germany) and kept under normal culture conditions (37°C, 5% CO_2, 95% humidity) until experimental use. After 1–4 days in culture, cells were thoroughly washed with PBS and pre-incubated for 30 min with CNR1 and CNR2 blockers AM251 and AM630, respectively, dissolved in DMEM/F-12 supplemented with 2% FCS and 1% P/S, and afterwards loaded with the Ca^{2+} sensitive fluorescence dye Fluoforte® (5 µM; Enzo Life Sciences, Lörrach, Germany) for another 30 min. After baseline measurement, equal volumes of the solvent EtOH or 30 µM CBD were acutely applied to the cells for 1 min. In a pilot experiment, using one pool of cultured human GCs (Day 3), derived from four individual follicular punctures, acute actions of CBD were challenged by pre-incubation and co-application of the TRPV2 inhibitor SET2 (10 µM; Tocris Bioscience), as described (Chai *et al.*, 2019). Carbachol (1 mM; Sigma-Aldrich) served as positive control and the application was done using a peristaltic pump (P720; Instech Laboratories, Plymouth Meeting, PA, USA). Fluorescence intensities (excitation 488 nm; emission 520 nm) were monitored under a confocal microscope (Axiovert 200M; Carl Zeiss, Jena, Germany) equipped with a laser module (LSM 5, Carl Zeiss) and a 20× objective (Plan-Apochromat 20x (0.8 NA), Carl Zeiss) using the AIM 4.2 software (Carl Zeiss). Based on arbitrary units (a.u.), background subtracted data are expressed as relative fluorescence intensity with a pseudo-color scale (black/purple—low Ca^{2+}; red/white—high Ca^{2+}).

Cytokine arrays

Supernatants originating from one pool of human GCs derived from five individual punctures and treated with 30 µM CBD or solvent control EtOH for 24 h were used for the Proteome Profiler Human XL Cytokine Array (R&D Systems, Minneapolis, MN, USA), to gain an overview of involved immunological factors linked to TRPV2 channel activation, as described earlier (Eubler

et al., 2018). According to the manufacturer's instructions, membranes were incubated with a total volume of 500 µl supernatant overnight at 4°C. Spot signal densities were determined by densitometry with the background subtracted and normalized to the corresponding protein concentration.

IL6 and IL8 immunoassays

Supernatants collected from human GCs treated for 24 h with 10 µM CBD, 30 µM CBD, or solvent control EtOH were evaluated for their IL6 (n = 7 for 10 µM; n = 6 for 30 µM) and IL8 levels (n = 6, each) using corresponding immunoassays (BMS204/3, Human IL8 Platinum ELISA, Invitrogen; BMS213/2, Human IL6 ELISA, Invitrogen), following the manufacturer's instructions. The lowest detectable concentration was 1.56 pg/ml for IL6 and 15.6 pg/ml for IL8, and the intra-assay coefficient of variance was <3.4% and 6.3%, respectively.

Proteome and secretome analysis

After completion of 24 h incubation with 30 µM CBD or solvent control EtOH started on cell culture Day 3, supernatants were collected and human GCs (n = 5, each) were washed thoroughly with PBS and detached from the culture dish using trypsin (BioChrom). Reactions were stopped using DMEM/F-12 supplemented with 10% FCS and 1% P/S, and the cell suspension was centrifuged at 800–1000 rpm (equivalent to ~230 g) for 3 min. The cell pellet was dissolved in 1 ml PBS for cell number determination using a Neubauer chamber and then washed in PBS twice. A total of 10^5 cells per sample were then lysed in a buffer consisting of 8 M urea (Carl Roth, Karlsruhe, Germany) in 50 mM ammonium bicarbonate (Riedel-de-Haën, Seelze, Germany) and sonicated (Sonoplus cup resonator, Bandelin, Berlin, Germany) for 15 min. Further lysis was done using QIAshredder homogenizers (QIAGEN) following the instructions of the manufacturer. Concentrations of proteins in the samples were measured (Bradford Assay; Thermo Fisher Scientific) and, for digestion, 10 µg of protein per sample were used. Cysteine residues were reduced with 1,4-dithiothreitol (5 mM for 30 min at 56°C). Alkylation was performed for 30 min at room temperature in the dark by the addition of iodoacetamide to give a concentration of 15 mM. Further, samples were quenched by 1,4-dithiothreitol (10 mM) for 15 min at room temperature. The digestion of proteins was performed in two steps: (i) lysyl-endopeptidase C (Lys C; Fujifilm Wako, Neuss, Germany) 1:100 enzyme/protein ratio, for 4 h at 37°C, and (ii) dilution of the samples with 50 mM ammonium bicarbonate to 1 M urea followed by overnight digestion with modified porcine trypsin (Promega, Madison, WI, USA) in a 1:50 enzyme/protein ratio at 37°C. For the secretome analysis, the supernatants were concentrated using Amicon centrifugal filters (2 ml, cutoff 10 kDa, Merck Millipore, Tullagreen, Carrigtwohill, Ireland). The volume was reduced to approximately 50 µl, and samples were adjusted to 1 M urea in 50 mM ammonium bicarbonate. They were centrifuged again to reduce the volume to ~50 µl. Digestion was performed as described above, without the dilution step. Nano LC-MS/MS analyses were carried out on an Ultimate 3000 RSLC instrument coupled to a Q Exactive HF-X mass spectrometer (Thermo Fisher Scientific). For analysis of the cellular proteome, 1.5 µg, and for secretome analysis, 750 ng were loaded onto a trap column (Acclaim™ Pepmap™ 100 C18, 100 µm × 2 cm, 5 µm, 100 Å, Thermo Fisher Scientific). LC separation of peptides was performed on an EASY-spray column (Acclaim™ Pepmap™ RSLC C18, 75 µm × 50 cm, 2 µm, 100 Å, Thermo Fisher Scientific). The flow rate was set to 250 nl/min. Solvent A consisted of 0.1% (v/v) formic acid in water. For the cellular proteomes, a two-step gradient from 3% B (0.1% (v/v) formic acid in acetonitrile) to 25% B in 160 min, followed by a ramp to 40% B for 10 min, was used. For the analysis of the secretome samples, a two-step gradient from 3% B to 25% B in 30 min, followed by a ramp to 40% B in 5 min, was applied. Mass spectrometry was performed in a data-dependent acquisition mode with a maximum of 15 MS/MS spectral scans per cycle.

Acquired MS spectra were then processed using MaxQuant (1.6.11.0), with the "match between runs" and the label-free quantification feature enabled (Tyanova et al. 2016). The Homo sapiens subset of the Swiss-Prot database was used for spectral search. Relative quantification, volcano plot analysis (Blighe and Lewis, 2022), principal component analysis (PCA), and heatmap generation were performed with Perseus v1.6.5.0 and R Statistical Software (v4.2.0; R Core Team 2021). For multiple testing correction and significance cut-off curve generation, the parameters were set to s0 = 0.1 and false discovery rate (FDR) <0.05. A gene set enrichment analysis (GSEA) using 4.2.3 version of (https://www.gsea-msigdb.org/gsea/index.jsp) was performed for annotation and functional enrichment analysis, with the following categories: GO_BP (biological process), KEGG and Reactome pathways. The results from GSEA were displayed using Cytoscape 3.9.1 software. The mass spectrometry data were deposited to the ProteomeXchange Consortium (www.proteomexchange.org, accessed on 3 October 2022) via the Proteomics Identification Database (PRIDE) partner repository with the dataset identifiers PXD041060 for both proteome and secretome data set (Perez-Riverol et al., 2022).

LDH assay

Supernatants collected from human GCs, and treated for 24 h with 10 µM CBD, 30 µM CBD, or corresponding solvent control EtOH, were examined for their LDH content as a sign of damaged cell membrane due to cytotoxic effects, as described previously (Blohberger et al., 2015). Using the Pierce LDH Cytotoxicity Assay Kit (Thermo Fisher Scientific) in accordance with the manufacturer's instructions, absorbance values of supernatants and a provided LDH positive control (positive ctrl.) were measured in duplicates at 490 and 690 nm (background) in a microplate reader (FLUOstar; BMG labtech, Ortenberg, Germany).

Progesterone measurements

Supernatants collected from human GCs treated for 24 h with 10 µM CBD, 30 µM CBD, or solvent control EtOH were examined for their progesterone content in a certified medical laboratory, i.e. Labor Becker MVZ GbR (Munich, Germany). Briefly, after HPLC separation (Shimadzu, Kyoto, Japan), samples were subjected to mass spectrometry analysis (QTRAP 6500+, Sciex, Toronto, Canada) to detect progesterone. Quantification was done on the basis of a six-point calibration method using commercially available calibrator solutions (<0.040–26 µg/l, 6PLUS1® Multilevel Serum Calibrator Set MassChrom® Steroid Panel 2, Chromsystems, Gräfelfing, Germany) and the results were verified with commercially available quality controls (MassCheck® Steroid Panel 2 Serum Controls, Chromsystems).

Data analysis and statistics

All mathematical and ensuing statistical analyses were performed by means of Microsoft Excel (2018, Microsoft, Redmond, WA, USA) and Prism 7 (GraphPad, San Diego, CA, USA). Statistical analysis of quantitative RT-PCR datasets was performed on the ΔCq values [ΔCq = Cq(target gen) – geometric mean Cq(housekeeping genes)] under control and treatment conditions

or from different culture days. For statistical analysis of IL6, IL8, or progesterone levels under control and treatment conditions, the measurements were normalized to the corresponding RNA amount or cell number. For western blots, the measured intensities of the TRPV2 and β-actin bands were background subtracted and their ratio (TRPV2/β-actin) was used for further analysis.

All datasets were then checked for outliers (ROUT method, Q = 1%) and Gaussian distribution (Shapiro–Wilk normality test, $\alpha = 0.05$), followed by a paired two-tailed t-test. For all the tests, α was set to 0.05 ($^{*}P \leq 0.05$, $^{**}P \leq 0.01$, $^{***}P \leq 0.001$), and data are presented as mean ± SEM.

Results

TRPV2 in the human and rhesus ovary and in cultured human GCs

We performed IHC experiments and readily identified TRPV2 in human and rhesus ovarian sections (Fig. 1A). Strong TRPV2 expression was seen in GCs, especially of antral follicles, and in the corpus luteum (CL) in both species. Further staining was also observed in endothelial cells, in theca cells, and in stromal cells, which may include immune cells. Sections incubated with antibody pre-adsorbed with a corresponding peptide, IgG or omission of primary antibody showed no staining.

To study this ovarian ion channel, we examined human GCs derived from IVF patients and transferred to cell culture, which is an adequate cellular model for large follicles and the CL. TRPV2 was readily detected in lysates of cultured human GCs by means of RT-PCR and western blot (Fig. 1B and Supplementary Figs S3 and S4A) and the results of ICC showed a scattered intracellular and membranous cellular expression pattern (Fig. 1C). Since these cells are known to rapidly change in culture, TRPV2 transcript and protein levels were examined in lysates derived from young (Days 1–2), intermediate (Days 3–4) and old (Days 5–6 for transcript; Days 5–7 for protein) cultured human GCs. The *TRPV2* transcript level of intermediate cultured human GCs (n = 9) was indistinguishable from that of young cells (n = 10), but it was significantly decreased in old cultured human GCs (0.6 ± 0.1-fold, $P = 0.002$; n = 9) (Fig. 2A). The same trend was observed for protein level (young and intermediate: n = 5; old: n = 4), but it did not reach statistical significance (Fig. 2B). Exposure of cultured human GCs to hCG (10 IU/ml; n = 17) or forskolin (FSK, 50 μM; n = 12), both involved in intracellular cAMP signaling,

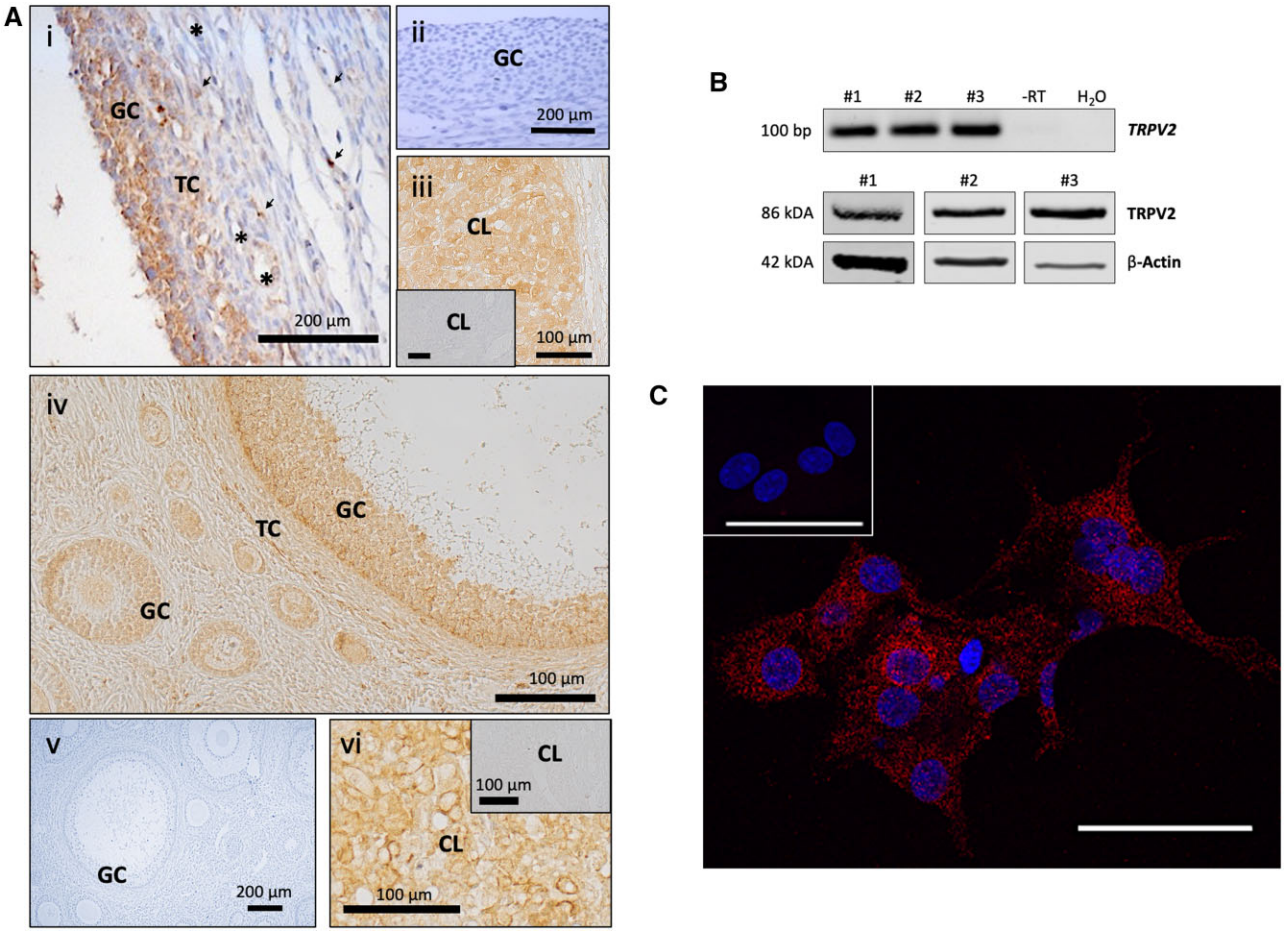

Figure 1. Expression of TRPV2 in the human and rhesus ovary and in cultured human GCs. (**A**) Ovarian sections from human (**i–iii**) and rhesus ovarian (**iv–vi**) tissue subjected to immunohistochemical staining against TRPV2, revealed strong expression in granulosa cells (GC) of small and big follicles, in theca cells (TC), in cells of the corpus luteum (CL), and in endothelial (asterisks) and stromal cells (arrow heads). Antigen pre-adsorbed TRPV2 antibody (ii), IgG control (v), and omission of the antibody (inserts of iii and vi), served as negative controls. (**B**) Cultured human GCs from independent isolations (n = 3) show TRPV2 expression at both the mRNA and protein levels, demonstrated by means of RT-PCR and western blot resulting in a 100 bp product and a single band of 86 kDa, respectively. For the RT-PCR, omission of the reverse transcriptase (-RT) or water (H_2O) instead of cDNA in the reaction served as negative controls; for the western blot, β-actin served as an internal loading control. (**C**) Cultured human GCs feature a scattered TRPV2 expression pattern. Scale bar 10 μm.

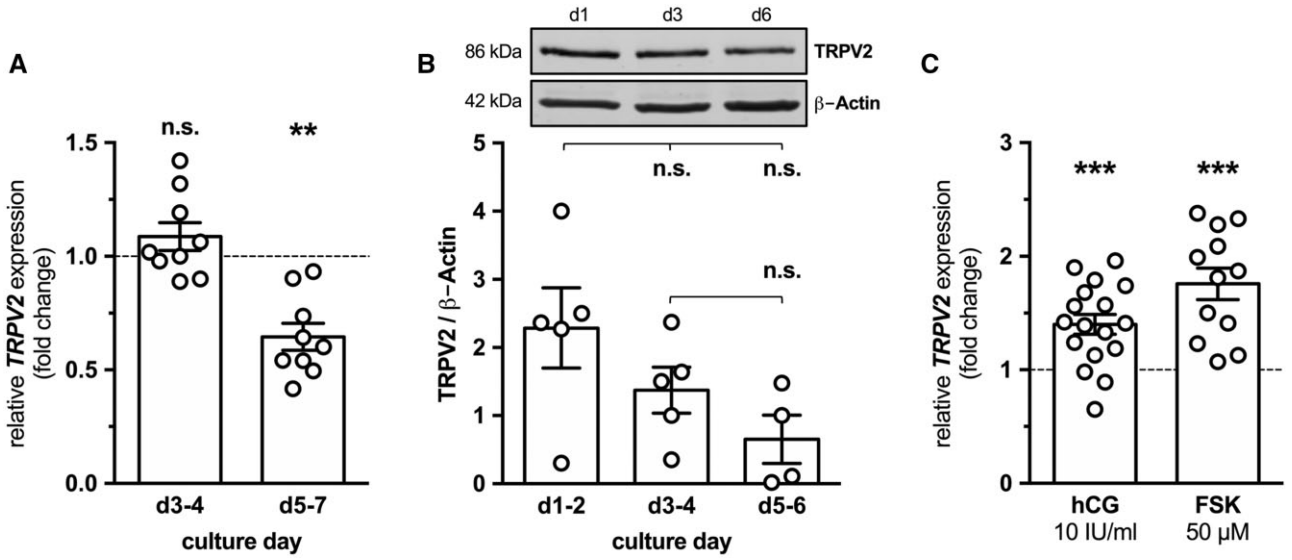

Figure 2. TRPV2 expression profile in view of culture days and cAMP signaling. (**A**) Relative *TRPV2* expression levels of human granulosa cells (GCs) cultured for 3–4 days (intermediate; n = 9) and for 5–7 days (old; n = 9) normalized to cells kept in culture for 1 day (young; n = 10). *TRPV2* expression levels were significantly lower in old cultured human GCs, whereas intermediate cells were indistinguishable from young ones. (**B**) TRPV2 immunoblotting of lysates derived from young (d1, n = 5), intermediate (d3–4, n = 5), and old cultured human GCs (d5–6, n = 4) revealed bands at the expected size of 86 kDa with decreasing but insignificant intensity in parallel to longer culture period. β-actin served as an internal loading control. Representative cropped original bands from young (d1), intermediate (d3), and old cultured human GCs (d6) are shown. (**C**) Relative *TRPV2* expression levels in cultured human GCs treated for 24 h with 10 IU/ml hCG (n = 17) or 50 µM FSK (n = 12), both involved in cAMP signaling, compared to cells treated with the corresponding solvent control PBS or ethanol (EtOH), each displayed a highly significant increase. Graphs represent the mean ± SEM and the individual data points; paired two-tailed *t*-test with $\alpha = 0.05$; n.s.: not significant, $^{**}P \leq 0.005$, $^{***}P \leq 0.001$.

significantly increased the *TRPV2* transcript levels by 1.4 ± 0.1-fold ($P < 0.001$) and 1.8 ± 0.1-fold ($P < 0.001$), respectively (Fig. 2C).

TRPV2 functionality in cultured human GCs

Channel functionality of TRPV2 as a non-selective cation channel was assessed by application of the agonist CBD in a calcium (Ca^{2+}) imaging set-up. To circumvent potential interference or activation of cannabinoid receptor 1 and 2 (CNR1/2), all experiments were performed in the presence of corresponding receptor blockers, i.e. AM251 (80 nM) and AM630 (800 nM).

Upon acute administration of 30 µM CBD for 1 min, cultured human GCs responded with transient Ca^{2+} influxes. However, the rate of responding cells and the kinetics of the resulting flux depended on the time spent in culture. With a responder rate of 88.2 ± 4.0% (67/76; n = 2), young cultured human GCs (Days 1–2) showed long-lasting, partially plateau-like Ca^{2+} fluxes (Fig. 3A and C), whereas intermediate cells, kept for 3–4 days in culture, displayed rather short increases of intracellular Ca^{2+} levels and a responder rate of 26.7 ± 6.7% (11/47; n = 2) (Fig. 3B and C). The reduced responder rate is in line with reduced *TRPV2* levels. Administration of an equal volume of the solvent control EtOH did not elicit any transient Ca^{2+} fluxes in any experiment. Responsiveness of cultured human GCs to carbachol (1 mM) was independent of time in culture and elicited intensive and plateau-like Ca^{2+} fluxes in 95.5 ± 3.2% (115/123; n = 4) of examined cells (Fig. 3A–C).

The specificity of these Ca^{2+} transients was verified in a pilot experiment using the recently published potent and selective TRPV2 agonist SET2 (Supplementary Fig. S5). One pool of cultured human GCs (culture Day 3) derived from four individual punctures responsive to 30 µM CBD (responder rate: 17.5%, 7/40; n = 1) did not show any responsiveness to SET2 alone and also not to co-application of both agents (responder rate: 0.0%, 7/40; n = 1). However, responsiveness to 1 mM carbachol was not affected (responder rate: 100.0%, 40/40; n = 1).

TRPV2 activation induces the expression and secretion of inflammatory factors in cultured human GCs

As TRPV2 is linked to inflammatory processes, supernatants derived from cultured human GCs treated on culture Day 3 with 30 µM CBD or solvent control EtOH for 24 h (n = 1) were subjected to a protein profiler assay to screen for regulated inflammatory factors (Fig. 4 and Supplementary Fig. S4B). The results showed that CBD-induced activation of TRPV2 increased secretion levels of cluster of differentiation 147 (CD147; 2.7-fold), C-X-C Motif chemokine ligand 1 (CXCL1; 14.0-fold), dipeptidyl-peptidase 4 (DPP4; 1.8-fold), and interleukin 8 (IL8; 5.8-fold), whereas thrombospondin 1 (THBS1; 0.43-fold) was decreased.

Next, mRNA extracts derived from cultured human GCs treated with different concentrations of CBD (1, 6, 10, and 30 µM) or corresponding solvent control EtOH for 4 or 24 h were subjected to quantitative RT-PCR (Fig. 5A and B and Supplementary Fig. S6). Short-term incubation for 4 h with 1 µM CBD (n = 5) induced significantly increased transcript levels of several inflammatory factors, i.e. *CD147* (1.3 ± 0.1-fold, $P = 0.007$), *IL8* (1.4 ± 0.1-fold, $P = 0.026$), monocyte chemo-attractant protein 1 (*MCP1*) (1.5 ± 0.1-fold, $P = 0.021$), and *THBS1* (1.4 ± 0.1-fold, $P = 0.021$). Upon application of 6 µM CBD for 4 h (n = 5), transcript levels of *IL8* (1.5 ± 0.2-fold, $P = 0.030$), *MCP1* (1.6 ± 0.2-fold, $P = 0.010$), and pentraxin 3 (*PTX3*) (1.6 ± 0.1-fold, $P = 0.004$) were significantly higher in comparison to solvent control-treated cells (Supplementary Fig. S6A). Administration of 10 µM CBD (n = 7) aggravated the increased transcript level of *MCP1* (2.0 ± 0.4-fold, $P = 0.039$), and, finally, 30 µM CBD (n = 7) resulted in an even more pronounced increase in transcript levels of several inflammatory factors, especially of cyclooxygenase 2 (*COX2*) (1.8 ± 0.2-fold, $P = 0.012$), *IL6* (1.9 ± 0.4-fold, $P = 0.029$), *IL8* (4.7 ± 0.2, $P = 0.002$), *MCP1* (2.0 ± 0.1-fold, $P < 0.001$), osteopontin (*OPN*) (1.6 ± 0.3-fold, $P = 0.048$), and *PTX3* (1.7 ± 0.2-fold, $P = 0.002$), in comparison to solvent control EtOH-treated cells (Fig. 5A).

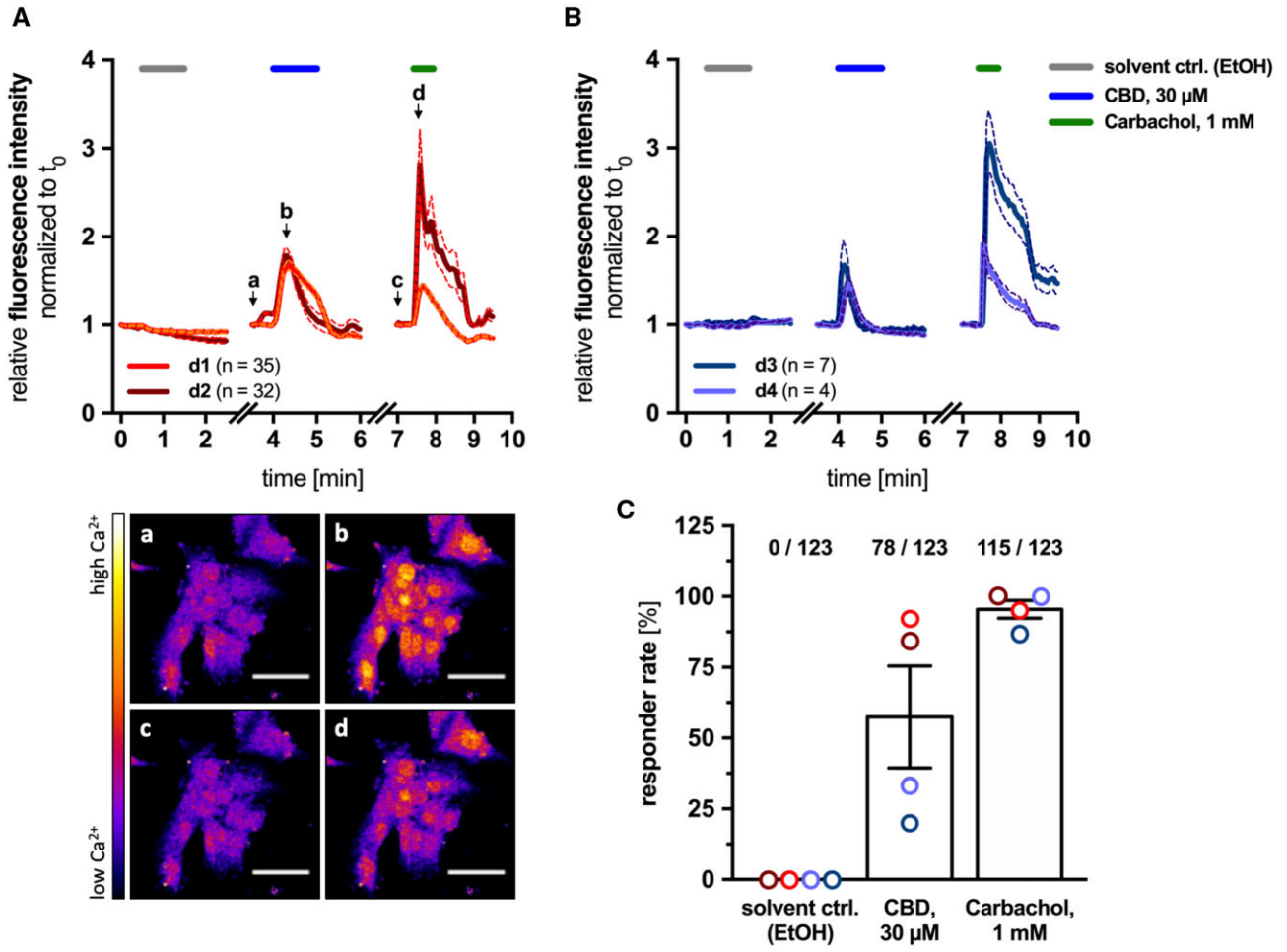

Figure 3. TRPV2 functionality assessed by means of calcium imaging. Functionality of TRPV2 as a non-selective cation channel was tested using a calcium imaging set-up and the TRPV2 activator cannabidiol (CBD). To circumvent potential activation and involvement of cannabinoid receptor 1 and 2 (CNR1/2), all experiments were performed in presence of corresponding blockers, i.e. AM251 (80 nM) and AM630 (800 nM). (**A**) Upon application of 30 µM CBD (blue line), young cultured human granulosa cells (GCs) (Days 1–2) responded with a transient, long-lasting and partially plateau-like increase in intracellular Ca^{2+} levels. (**a**–**d**) Representative live cell images at the indicated timepoints (arrows in A) as pseudo-color images representing high Ca^{2+} levels in red and low Ca^{2+} levels in purple/black, respectively. (**B**) In intermediate cultured human GCs (d3–4), 30 µM CBD induced a rather short increase of intracellular Ca^{2+} levels. The solvent control ethanol (EtOH) (grey line) did not elicit any transients in any experiment, administration of 1 mM Carbachol (green line) served as positive control and resulted in sustained plateau-like Ca^{2+} transients. Each graph shows averaged original traces (solid line) and dedicated SEM (dashed line); cell numbers are given in the corresponding legends. (**C**) Responder rate of cultured human GCs manifested to depend on time in culture, with a higher responder rate in young (67/76; light/dark red, n = 2) than in intermediate cells (11/47; light/dark blue, n = 2). The responsiveness to 1 mM Carbachol was not dependent on culture time (115/123; n = 4), as was the insensitivity of cultured human GCs to the solvent control EtOH (0/123, n = 4).

Prolonged exposure to these CBD concentrations for 24 h resulted in a yet further increase in transcript levels of inflammatory factors, additionally pointing to a time dependency in TRPV2 mediated effects. As such, especially *COX2* (5.9 ± 2.4-fold, $P < 0.001$), *CXCL1* (3.2 ± 0.9-fold, $P = 0.004$), *IL6* (4.0 ± 1.3-fold, $P < 0.001$), *IL8* (7.6 ± 2.8-fold, $P < 0.001$), and *PTX3* (9.4 ± 2.9-fold, $P < 0.001$) were highly significantly elevated after 24 h treatment with 30 µM CBD (n = 21) (Fig. 5B and Supplementary Fig. S6B).

To examine whether the observed increased *IL6* and *IL8* transcript levels mirror elevated protein levels, supernatants derived from cultured human GCs treated for 24 h with 10 µM CBD, 30 µM CBD or corresponding solvent control EtOH were analyzed using ELISAs (Fig. 5C and D). Whereas administration of 10 µM CBD resulted in increased but not statistically significant changes in IL6 secretion levels (2.6 ± 0.8-fold, $P = 0.063$, n = 7), the basal IL8 levels were significantly raised from 45.8 ± 10.7 pg/ml to 233.2 ± 61.2 pg/ml (1.7 ± 0.3-fold, $P = 0.049$, n = 6). Secreted levels of both IL6 (5.5 ± 1.3-fold, $P = 0.018$) and IL8 (3.3 ± 0.5-fold, $P = 0.007$) were significantly increased in supernatants derived from cultured human GCs treated for 24 h with 30 µM CBD (n = 6, each).

TRPV2 activation interferes with steroidogenic properties of cultured human GCs

Since GCs produce and secrete steroids, a potential impact of TRPV2 activation on steroidogenic properties of cultured human GCs was assessed. While short-term incubation with 1 µM (n = 5), 6 µM CBD (n = 5), 10 µM or 30 µM CBD (n = 7, each) had almost no effect on transcript levels of cytochrome p450 family 19 subfamily a member 1 (*CYP19A1*), P450 side-chain cleavage (*P450scc*) or steroidogenic acute regulator (*StAR*) (Supplementary Fig. S6C and Fig. 6A), prolonged exposure to CBD for 24 h resulted in significantly reduced transcript levels of all examined genes in a dose-dependent manner (30 µM: *CYP19A1*—0.9 ± 0.1-fold, $P < 0.001$; *P450scc*—0.6 ± 0.1-fold, $P < 0.001$; *StAR*—0.7 ± 0.1-fold, $P = 0.017$; n = 21) (Supplementary Fig. S6D and Fig. 6B). In line with this

observation, the progesterone content in supernatants derived from cultured human GCs treated with 10 µM CBD was significantly decreased (0.8 ± 0.1-fold, $P = 0.038$, n = 6) compared to supernatants obtained from cells treated with the solvent control, i.e. EtOH-treated cells (Fig. 6C). The treatment with 30 µM CBD evoked the same trend but did not reach statistical significance (0.8 ± 0.2-fold, $P = 0.118$, n = 6).

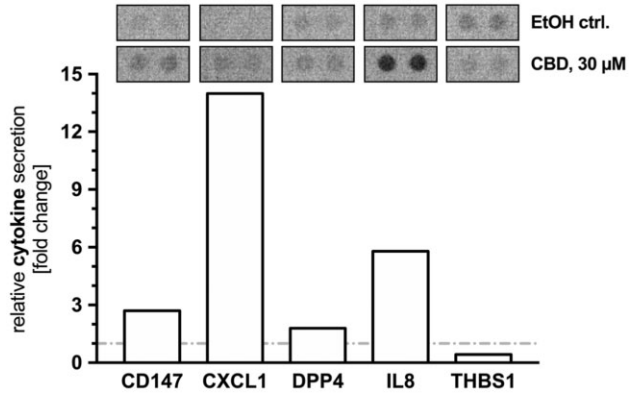

Figure 4. TRPV2 activation investigated by means of a proteome profiler. Supernatants of cultured human granulosa cells (GCs) treated with 30 µM cannabidiol (CBD) or solvent control ethanol (EtOH) for 24 h (n = 1) were investigated for their cytokine and chemokine content, using a Human Proteome Profiler. Administration of 30 µM CBD to cultured human GCs on culture Day 3 induced increased secretion levels of CD147, CXCL1, DPP4, and IL8, whereas THBS1 was decreased. Corresponding membrane spots are depicted on top of each column, upper row solvent control EtOH (EtOH ctrl.) and lower row 30 µM CBD (CBD, 30 µM).

Impact of TRPV2 activation on proteome and secretome of cultured human GCs

Next, a proteomic analysis was performed on lysates and corresponding supernatants of cultured human GCs treated with 30 µM CBD or solvent control EtOH for 24 h on culture Day 3 (n = 5). In total, 5094 proteins and 57,308 peptides were identified in the proteomes and 424 proteins, and 1482 peptides were identified in the secretomes. The entire list of identified proteins is available as MaxQuant proteinGroups.txt file at the PRIDE repository (https://www.ebi.ac.uk/pride/) with the dataset identifier PXD041060. PCA of proteomes showed a slight separation between cultured human GCs treated with 30 µM CBD or solvent control EtOH (Fig. 7A), whereas no separation between the corresponding secretomes could be observed (Supplementary Fig. S7A). To analyze the effects of CBD-mediated TRPV2 activation and to elucidate proteomic differences between CBD-treated cultured human GCs and solvent control EtOH-treated cells, a volcano plot analysis of the proteome and secretome data sets was performed. Student's *t*-test with permutation-based FDR correction ($q < 0.05$) resulted in 14 differentially abundant proteins, of which 6 proteins were more abundant and 8 proteins less abundant in the proteomes of CBD-treated cells (Fig. 7B). Furthermore, the dendrogram of the heatmap of Z-scored differentially abundant protein values displayed clusters of cells treated with 30 µM CBD or solvent control EtOH (Fig. 7C). Volcano plot analysis for secretomes resulted in two proteins with increased abundance in

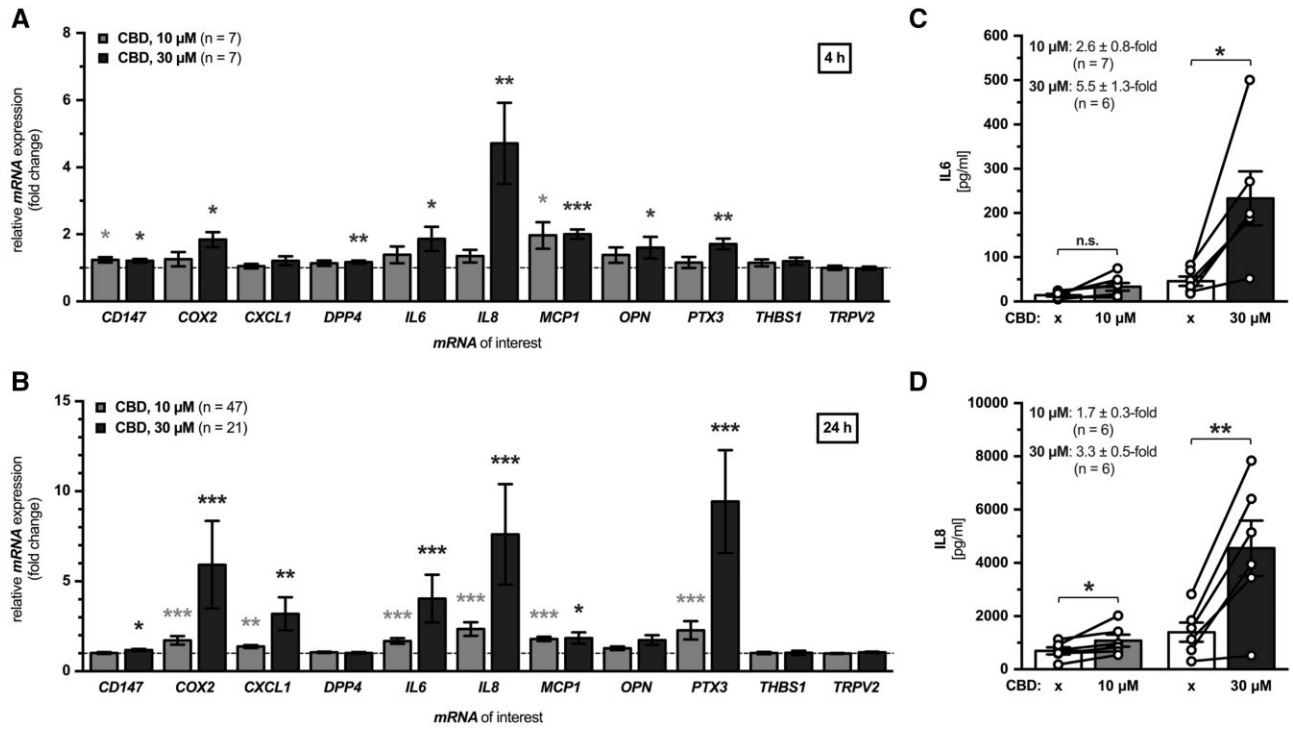

Figure 5. Inflammatory TRPV2 actions examined by means of quantitative RT-PCR and ELISA. (**A**) Cultured human granulosa cells (GCs) treated on culture Day 3 for 4 h with 10 or 30 µM cannabidiol (CBD) (n = 7, each) exhibited a dose-dependent increase in mRNA levels of several factors, such as *COX2*, *IL6*, *IL8*, *MCP1*, *OPN*, and *PTX3*, in comparison to the corresponding solvent control ethanol (EtOH). (**B**) Prolonged exposure to 10 µM (n = 47) or 30 µM CBD (n = 21) for 24 h intensified this increase in inflammatory gene expression, especially for *COX2*, *IL6*, *IL8*, and *PTX3*. (**C**) IL6 immunoassay revealed increased secretion levels upon 24 h treatment of cultured human GCs with 10 µM (n = 7) or 30 µM CBD (n = 6) compared to the corresponding solvent control EtOH (x), whereas only the treatment with 30 µM CBD resulted in significantly more IL6 in the supernatant. (**D**) Supernatant levels of IL8 were significantly increased after 24 h incubation with both 10 µM and 30 µM CBD (n = 6, each), compared to the solvent control EtOH (x). Graphs represent the mean ± SEM and the individual data points for ELISA measurements; paired two-tailed t-test with $\alpha = 0.05$; n.s.: not significant, $^{*}P \leq 0.05$, $^{**}P \leq 0.005$, $^{***}P \leq 0.001$.

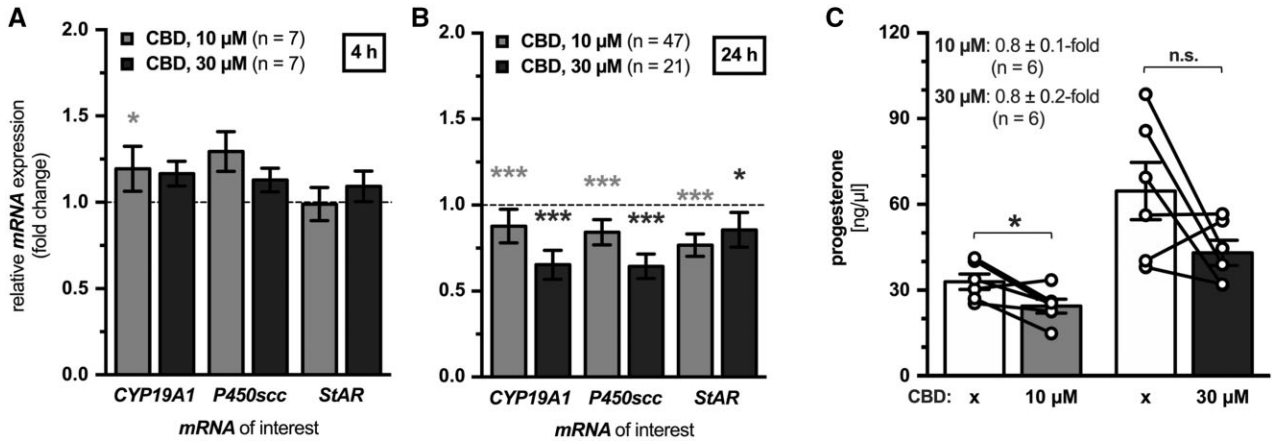

Figure 6. TRPV2 activation and steroidogenic profile of cultured human granulosa cells (GCs). The potential impact of TRPV2 activation on mRNA levels of steroidogenic genes and on progesterone production was examined. (**A**) In cultured human GCs treated for 4 h with 10 or 30 µM cannabidiol (CBD) (n = 7, each) on culture Day 3, mRNA levels of *P450scc* and *StAR* were unaffected, whereas 10 µM CBD induced a slightly significant increase in *CYP19A1*, compared to solvent control ethanol (EtOH) treated cells. (**B**) After 24 h of incubation with 10 µM (n = 47) or 30 µM CBD (n = 21), all three investigated mRNAs were significantly lower. (**C**) The progesterone content in the supernatants after 24 h incubation with 10 µM CBD was slightly but significantly reduced in comparison to solvent control EtOH (x) treated cells (n = 6). The treatment with 30 µM CBD showed a trend to lower values, which was however not statistically significant (n = 6). Graphs represent the mean ± SEM and the individual data points for progesterone measurements; paired two-tailed *t*-test with $\alpha = 0.05$; n.s.: not significant, $^{*}P \leq 0.05$, $^{**}P \leq 0.005$, $^{***}P \leq 0.001$.

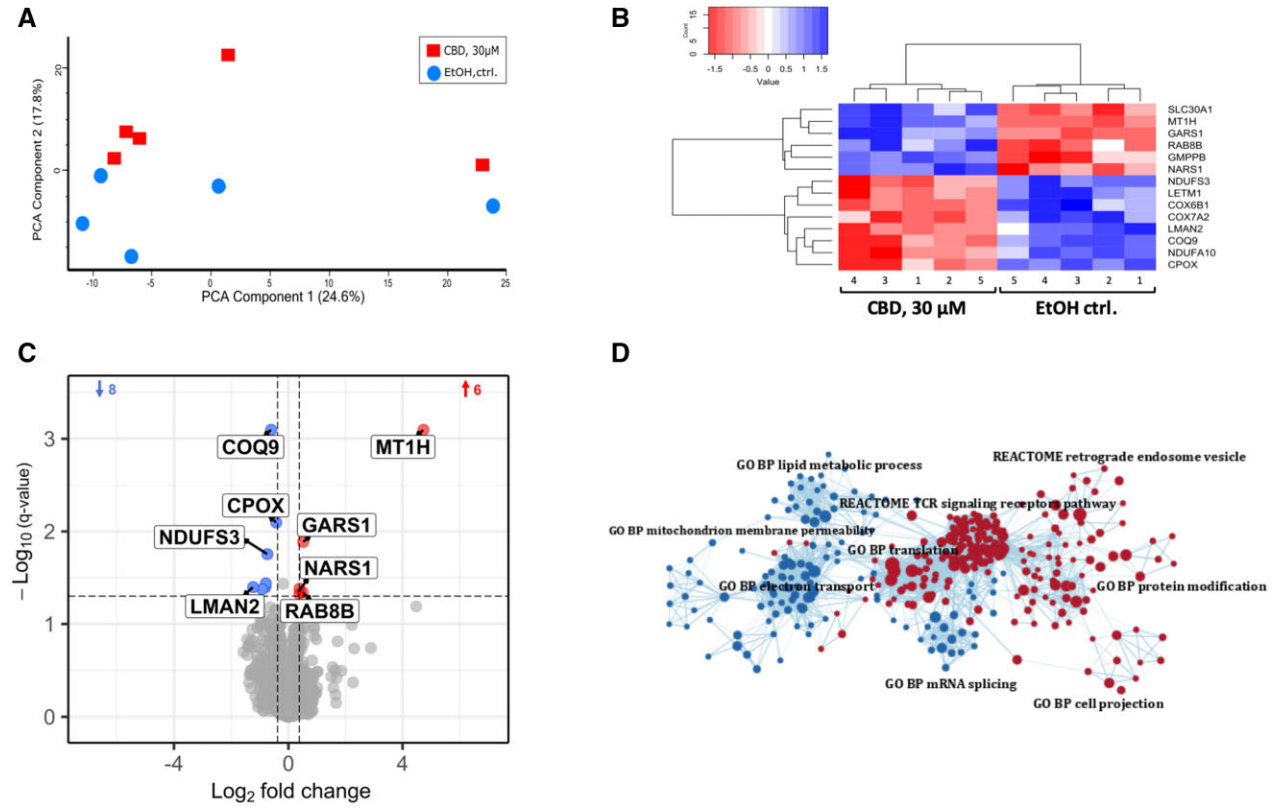

Figure 7. TRPV2 activation examined by means of quantitative proteome analysis. To gain an even deeper insight into TRPV2-mediated actions in these ovarian cells, cultured human granulosa cells (GCs) of culture Day 3 treated for 24 h with 30 µM cannabidiol (CBD) or solvent control ethanol (EtOH) (n = 5) were subjected to mass spectrometry. (**A**) Principal component analysis (PCA) of cellular proteomes. Each data point depicts a single biological replicate. Colors and shapes represent the experimental group. (**B**) Volcano plot analysis for proteomes of cultured human GCs treated with 30 µM CBD in comparison to solvent control EtOH-treated cells. (**C**) Heat map and unsupervised hierarchical clustering of intensity profiles of the differentially abundant proteins after *Z*-scoring. (**D**) Gene set enrichment analysis of quantified proteins. Results with $q < 0.05$ were considered significant and were visualized. Categories used for the analysis were: GO biological process, reactome pathways, and KEGG pathways.

CBD-treated cells (Supplementary Fig. S7B). A list of differentially abundant proteins is available in Table 2.

Additionally, a GSEA for the entire data set was done to perform a statistical analysis at the level of related functional terms rather than at the level of individual proteins. The analysis of the proteomic data sets resulted in 362 enriched gene sets, whereof 293 were increased and 69 were decreased (FDR <0.05). The most prominent gene sets within the proteins more abundant in

Table 2. List of differentially abundant proteins in cellular proteomes and secretomes.

Gene name	Protein name	Log2 FC	q value	Gene Ontology (GO) biological process (Uniprot)
More abundant in cellular proteomes				
MT1H	Metallothionein-1H	4.72	0	Metal binding
SLC30A1	Zinc transporter 1	0.94	0.03	Zinc transport, ion transport
GARS1	Glycine-tRNA ligase	0.51	0.013	Protein biosynthesis
RAB8B	Ras-related protein Rab-8B	0.50	0.04	Protein transport, transport
NARS1	Asparagine-tRNA ligase, cytoplasmic	0.39	0.04	Protein biosynthesis
GMPPB	Mannose-1-phosphate guanyltransferase beta	0.38	0.04	protein glycosylation
Less abundant in cellular proteomes				
LETM1	Mitochondrial proton/calcium exchanger protein	−0.19	0.03	Calcium transport, ion transport
CPOX	Oxygen-dependent coproporphyrinogen-III oxidase	−0.42	0.01	Heme biosynthesis, porphyrin biosynthesis
COQ9	Ubiquinone biosynthesis protein COQ9	−0.60	0	Ubiquinone biosynthesis
NDUFS3	NADH dehydrogenase [ubiquinone] iron-sulfur protein 3	−0.74	0.01	Electron transport, respiratory chain, transport
COX7A2	Cytochrome *c* oxidase subunit 7A2	−0.79	0.03	Cellular respiration, mitochondrial electron transport, cytochrome *c* to oxygen
NDUFA10	NADH dehydrogenase [ubiquinone] 1 alpha subcomplex subunit 10	−0.80	0.04	Electron transport, respiratory chain, transport
COX6B1	Cytochrome *c* oxidase subunit 6B1	−0.91	0.04	Cellular respiration, mitochondrial electron transport, cytochrome *c* to oxygen
LMAN2	Vesicular integral-membrane protein VIP36	−1.23	0.04	Protein transport, transport
More abundant in secretomes				
P4HB	Protein disulfide-isomerase	1.93	0.01	Interleukin-12-mediated signaling pathway, positive regulation of cell adhesion, response to endoplasmic reticulum stress
CAPZA1	F-actin-capping protein subunit alpha-1	2.03	0.08	Actin cytoskeleton organization

cultured human GCs treated with 30 μM CBD were related to T-cell receptor signaling receptor pathways and to translation. Strikingly, enriched terms from the set of less abundant proteins in CBD-treated cells were related to electron transport, mRNA splicing and lipid metabolic process (Fig. 7D). GSEA was also performed for the secretome data set but did not result in any significantly enriched gene sets.

TRPV2 activation has no cytotoxic effects in cultured human GCs

To examine the possibility that the observed proteomic changes, especially those hinting to changes in electron transport, may reflect cytotoxic effects of the treatment with CBD, supernatants collected from cultured human GCs treated for 24 h with 10 μM CBD, 30 μM CBD or corresponding solvent control EtOH (n = 7, each) were examined for their LDH content, as a sign of damaged cell membrane. The measured absorbance values did not differ between supernatants derived from CBD or solvent control EtOH-treated cultured human GCs (10 μM: $P = 0.431$; 30 μM: $P = 0.427$; Supplementary Fig. S8).

Discussion

In our previous studies, TRPV2 was identified as a mediator of inflammatory processes in peritubular cells of the male human gonad (Eubler *et al.*, 2018) and, due to its expression in murine testicular macrophages, was linked to testicular dysfunction and infertility caused by an inflammatory cascade in a mouse model of infertility (aromatase transgenic mice; Eubler *et al.*, 2021).

The present study introduces, for the first time, the non-selective cation channel TRPV2 as an ion channel of the human and non-human primate ovary. Expression was detected in several ovarian cells, including GCs situated in large antral follicles, in the CL, in theca cells, endothelial cells, and stromal cells, presumably immune cells. These sites match well the expression sites documented in the Human Protein Atlas (https://www.proteinatlas.org/ENSG00000187688-TRPV2/single+cell+type/ovary). Of note, this channel is abundantly present in isolated human GCs derived from patients undergoing medical reproductive procedures and transferred to cell culture conditions, as documented by the data of previous proteomic studies (Bagnjuk *et al.*, 2019; Beschta *et al.*, 2021). The experimental focus was therefore on isolated human GCs and in these cells, TRPV2 expression levels were dependent on the time in culture and on the concentration of the hormone hCG and cAMP. Channel functionality was demonstrated by acute application of the known agonist CBD and resulted in transient Ca^{2+} influxes. Furthermore, these CBD-induced transients were abolished in the presence of the selective TRPV2 antagonist SET2, pinpointing the involvement of TRPV2. Consequences of prolonged exposure to CBD included higher expression and secretion, respectively, of several inflammatory factors, i.e. *COX2*, *IL6*, *IL8*, and *PTX3*. In parallel, the production of progesterone was inhibited and subtle changes in cellular proteomes became evident. The data imply roles of TRPV2 in the human ovary.

The choice to use CBD as a pharmacological activator of TRPV2 in this and in previous studies (Eubler *et al.*, 2018, 2021) is based on the reports that it is a preferential activator of TRPV2 (Qin *et al.*, 2008; De Petrocellis *et al.*, 2011; Pumroy *et al.*, 2019;

Landucci *et al.*, 2022). Furthermore, in two previous proteomic studies of cultured human GCs, in which up to 5962 GC proteins were identified (Bagnjuk *et al.*, 2019; Beschta *et al.*, 2021), TRPV2 was readily detected.

Yet, we are aware that CBD also can interact with other targets (Ibeas Bih *et al.*, 2015). Such targets include, among others, the cannabinoid receptors, CNR1 and CNR2, respectively. Neither one is, however, present in the proteomic data of cultured human GCs (Bagnjuk *et al.*, 2019; Beschta *et al.*, 2021; Supplementary Fig. S9A). Based on the data of the Human Protein Atlas (https://www.proteinatlas.org/ENSG00000118432-CNR1/single+cell+type/ovary) and https://www.proteinatlas.org/ENSG00000188822-CNR2/single+cell+type/ovary; accessed on 15 June 2023), expression of *CNR1* and *CNR2* is detected mainly in human ovarian smooth muscle, stromal, and endothelial cells. The gene expression data are thus in complete contrast to earlier data, which were based on immunohistochemical results. The study described stronger CNR2 than CNR1 immuno-reactivities in GCs of follicles and cells of the CL and corpus albicans (El-Talatini *et al.*, 2009). Nevertheless, to rule out interference of CBD with such receptors in cultured human GCs, all experiments reported in our study were performed in the presence of respective blockers, as described earlier (Eubler *et al.*, 2018, 2021).

The calcium channels $Ca_V3.1$ and $Ca_V3.2$ can also be targeted by CBD (Ibeas Bih *et al.*, 2015). Although they were described in human GCs (Agoston *et al.*, 2004), interactions of CBD with both result in the inhibition of these channels (Ross *et al.*, 2008). Hence, they most likely do not participate in the action of CBD to elevate Ca^{2+} in GCs.

Provided that they are present in human GCs, further membrane receptors and ion channels might possibly be targeted by CBD, according to previous data (Ibeas Bih *et al.*, 2015). They may include glycine and opioid receptors, GPR18 and GPR55, 5-HT1A and 2A, PPRG, and CHNRA7. To our knowledge glycine receptors are not linked to elevations of Ca^{2+} and most are inhibited by CBD (GPR18, GPR55, opioid receptors, CHNRA7), while the interactions of CBD with others (PPRG) are not well defined. Of note, none of these were detected when we searched data sets of proteome analyses of cultured human GCs (Bagnjuk *et al.*, 2019; Beschta *et al.*, 2021; Supplementary Fig. S9A).

This negative result does not completely rule out their presence in GCs, but implies protein levels too low to be detectable by MS. This possibility is indicated by the results of a search for the presence of corresponding transcripts in the Human Protein Atlas and yet another transcriptomic data set (Zhang *et al.*, 2018; Supplementary Fig. S9B). Here we found evidence for presence (*PPARG*), low levels (*CNR1*, *GLYR1*, *GPR18*, *CHRNA7*), or absence (*CNR2*, *GPR55*, *5-HT1A/-2A*, opioid receptors) of such transcripts.

With respect to other TRP channels (TRPA1, TRPM8, TRPV1; TRPV3, TRPV4; Ibeas Bih *et al.*, 2015), which may be possible channel targets of CBD and are more closely related to TRPV2, again none of these were detected when we searched proteomic data sets with up to 5962 proteins of cultured human GCs (Bagnjuk *et al.*, 2019; Beschta *et al.*, 2021). When we searched for transcripts, we found some evidence for *TRPV1*, *TRPV3*, and *TRPV4* in the single cell data set of the Human Protein Atlas (accessed June 12, 2023), whereas next to TRPV2, only TRPV1 and TRPV4 were detected in the study of Zhang and colleagues (Zhang *et al.*, 2018; Supplementary Fig. S10A). We also performed RT-PCR studies in cultured GCs and detected *TRPA1*, *TRPV1*, and *TRPV4* transcripts. In agreement with the previous proteomic results, a western blot for TRPV1 did not detect an immunoreactive band (Supplementary Fig. S10B–D).

Thus, we cannot rule out that some of these channels may be expressed at levels too low to be detectable by mass spectrometry or western blotting in human GCs but have reason to assume that they are not involved in mediating the actions of CBD. In contrast, TRPV2 is readily detectable, as mentioned, by mass spectrometry (Bagnjuk *et al.*, 2019; Beschta *et al.*, 2021) and western blotting, clearly indicating that it is highly abundant. In addition, a blocker of TRPV2, SET2, abolished the CBD-induced increase in Ca^{2+}, thus further pinpointing TRPV2 as the main CBD target in human GCs.

Other mainly (intra)cellular proteins were found in different assays to be targeted by CBD (Ibeas Bih *et al.*, 2015). Most of them exist in many cell types, e.g. SOD, catalase, enzymes involved in xenobiotic metabolism, ceramide synthesis, electron transport chain, and many others (see summary in Ibeas Bih *et al.*, 2015). While possible interactions of CBD with such proteins in GCs remain to be studied, such interactions are however unlikely to be involved in the acute actions of CBD, namely, to elevate Ca^{2+} in GCs.

Inflammatory processes are of fundamental importance for ovarian folliculogenesis, ovulation, and tissue remodeling, e.g. after oocyte expulsion. Although the current knowledge about the precise actions of secreted cytokines is still limited, they are by now considered key to reproductive success, creating, for example, an immune-permissive and embryotrophic environment (Field *et al.*, 2014). Known inflammatory factors include IL1β, IL6, IL8, MCP1, and tumor necrosis factor alpha (TNF-α). Their presence strongly depends on different developmental stages during folliculogenesis and luteinization (Buyalos *et al.*, 1992; Wang *et al.*, 1992; Machelon *et al.*, 1995; Büscher *et al.* 1999; Dahm-Kahler *et al.*, 2009; Field *et al.*, 2014). Increased expression of COX2 and consequently elevated prostaglandin synthesis and prostaglandin actions accompany, and are essential for, ovulation (Richards *et al.*, 2008; Trau *et al.*, 2016; Duffy *et al.*, 2019). However, while being of physiological importance, imbalanced or chronically elevated inflammatory factors are associated with altered ovarian function. This is known to occur in conditions such as obesity and PCOS, for instance (Espey 1980, 1994; Boots and Jungheim, 2015; Adams *et al.*, 2016).

It is not possible to directly study these events in the human ovary, yet human GCs from preovulatory follicles are an apt model for the human ovary, specifically for the large/antral periovulatory follicle and the CL (Bagnjuk and Mayerhofer, 2019). Cultured human GCs possess the enzymatic repertoire for progesterone production, i.e. 3β-hydroxysteroid dehydrogenase (3β-HSD), CYP11A1 and StAR (Bagnjuk and Mayerhofer, 2019), and sex-steroid production by GCs, is regulated by luteinizing hormone (LH) or hCG, which both bind to the LH/choriogonadotropin receptor (LHCGR) and activate downstream signaling pathways including protein kinase A (PKA), protein kinase C (PKC), and phosphatidylinositol 3-kinase (PI3K). Interestingly, the set of activated and induced genes is not only relevant in various aspects of ovulation, but the encoded proteins are also routinely associated with inflammation (Boots and Jungheim, 2015; Duffy *et al.*, 2019). Moreover, all these kinases are also known to modulate cellular localization and to potentiate the responsiveness of TRPV2 (Kanzaki *et al.*, 1999; Nagasawa *et al.*, 2007; Link *et al.*, 2010), which, on top of that, also features a strong link to inflammatory processes (Santoni *et al.*, 2013). Although, for example, potentiation of channel responsiveness and a possible influence on the subcellular localization remain to be investigated in cultured human GCs, our study shows that elevated cAMP levels upon hCG and FSK application resulted in significantly increased transcript

levels of TRPV2 and that channel activation entailed the induction of inflammatory factors in these ovarian cells.

The two factors upregulated most upon TRPV2 activation, and confirmed by ELISA measurements, were IL6 and IL8. We focused on these two, also because both are well known in the female reproductive tract and, as such, both have been associated with positive pregnancy outcomes in several studies (Field et al. 2014). IL6 is also postulated to have an autocrine regulatory function in the ovary, inducing expression of genes involved in cumulus-cell expansion and extracellular matrix formation, such as PTX3, which may explain our observation of the CBD-induced increase in *PTX3* levels. The angiogenic and chemoattractant/chemotactic factor IL8 is important for follicle maturation and levels increase in parallel to follicle size (Brännström and Norman, 1993; Arici et al., 1996; Runesson et al., 1996; Kawano et al., 2012). The main sites of follicular IL8 production are theca cells of late-follicular/early-ovulatory follicles, but also GCs around the time of ovulation (Arici et al., 1996). IL8, besides improving peri-follicular blood flow in concert with MCP1, is essential for the recruitment and activation of leukocytes required for ovulation (Brännström and Norman, 1993; Arici et al., 1996, 1997; Murayama et al., 2010). In line with this, we also observed increased *MCP1* transcript levels in response to CBD-induced TRPV2 activation in cultured GCs. The results of our study lead us to propose that TRPV2 is an overlooked player in these physiological events.

Furthermore, as increased levels of IL6 and IL8 are reported in PCOS (Adams et al., 2016), our study also raises the possibility that TRPV2 may be involved in ovarian pathologies, which may also include ovarian hyperstimulation syndrome. The patients feature characteristically low progesterone levels, which are linked to high IL6 levels in the follicular fluid (Loret de Mola et al., 1996).

We also found that *COX2* transcripts were increased upon TRPV2 activation, implying increased prostaglandin production by GCs. This possibility was, however, not further studied in the present study. Elevated prostaglandins are crucial for ovulation (Duffy et al., 2019); therefore, additional detailed follow-up studies addressing prostaglandins, as well as other regulated factors, e.g. OPN or THBS1, are now required.

To explore other potential TRPV2 actions, we performed a proteome analysis. Of the identified set of proteins affected by CBD treatment or TRPV2 activation, only a few have been linked to the human ovary before, and therefore, their ovarian roles are not or not well established. This pertains to, for example, Coenzyme Q9 (COQ9), Cytochrome C Oxidase Subunit 6B1 (COX6B1), and Metallothionein 1 (MT1). Both COQ9 and COX6B1 are involved in mitochondrial electron transport system and are thus essential for energy metabolism. In addition, they have been linked to oocyte quality in humans and cattle (Ortega et al., 2017; Qi et al., 2020). Of note, in PCOS patients, *COX6B1* transcript levels, among other mitochondrial genes, were revealed to be prematurely increased in oocytes at the germinal vesicle stage and may contribute to the declining oocyte quality in these patients (Qi et al., 2020). In cattle, missense mutations in the COQ9 gene yielded higher oocyte mitochondrial content and improved fertility (Ortega et al., 2017). MT1, which is present in the theca interna of preovulatory and in luteinized GCs of postovulatory follicles in rats (Espey et al., 2003), is associated with metal and immune homeostasis regulation. It can be induced by several factors, including inflammatory cytokines including interferon gamma (IFN-γ), IL6, and TNF-α, but also the bacterial endotoxin lipopolysaccharide (LPS) (De et al., 1990; Dai et al., 2021). Together with upregulated MT1 expression, bacterial infections also result in increased levels of solute carrier family 30 member 1 (SLC30A1) (Botella et al., 2011), which was also found to be altered upon CBD treatment of cultured human GCs. Interestingly, LPS also acts agonistically at TRPV2 (Yamashiro et al., 2010). Further proteins increased in CBD-treated samples are glycine-tRNA ligase (GARS1) and asparagine-tRNA ligase (NARS1), which play an essential role in protein synthesis (Wang et al., 2020; Sung et al., 2022). These proteins are expressed in follicle cells and ovarian stroma cells (https://www.proteinatlas.org/ENSG00000106105-GARS1/tissue/ovary, https://www.proteinatlas.org/ENSG00000134440-NARS1/tissue/ovary; accessed on 15 March 2023). Their function in the ovary is not well examined. However, recent studies have identified both proteins as potential biomarkers for ovarian cancer (Alexandrova et al., 2020).

The data identified changes in mitochondrial proteins and hence, we performed a screen for cell death. Yet, cell death, as a possible consequence of CBD treatment is unlikely, as CBD did not affect LDH levels in the cell culture medium.

A question that cannot be answered easily at this time is what is/are the physiological activator(s) of TRPV2 in the ovary and GCs? Several possibilities are to be considered.

As mentioned, TRPV2 is reported to be activated by mechanical forces and by ROS (Caterina et al., 1999; Neeper et al., 2007; Qin et al., 2008; Monet et al., 2009; Shibasaki et al., 2010; Zhang et al., 2012; Kojima and Nagasawa, 2014; Shibasaki, 2016; Oda et al., 2021). These modes of activation must be considered, alone or, more likely, in combination for ovarian TRPV2, in particular. Whether and how ROS levels normally increase in the growing follicle is not well known, as these volatile, short-lived molecules are dynamically being produced and degraded (Ávila et al., 2016; Buck et al., 2019). Ovarian tissue stiffness changes when follicles grow (Biswas et al., 2022; Fiorentino et al., 2023) and, specifically, intrafollicular pressure changes in the growing and preovulatory follicle have been reported (Matousek et al., 2001). Given that the expression of TRPV2 in GCs also increases with follicle size, we speculate that TRPV2 may act as an ovarian mechanosensor. It might be a bridging element between the increasing intrafollicular pressure during follicle growth, initially considered the key for follicle rupture (Asdell, 1962), and the LH-induced inflammatory processes, nowadays a generally accepted key aspect for ovulation (Espey 1980, 1994; Duffy et al., 2019).

Additional activators of ovarian TRPV2 may be growth factors, as TRPV2 has initially been described as a growth factor-regulated channel due to its responsiveness to insulin-like growth factor I (IGF1) (Kanzaki et al., 1999). Several studies have shown a correlation between higher follicular fluid levels of IGF1 and better oocyte and embryo quality and higher implantation rates (Molka et al., 2022). This chain of events could include actions of TRPV2.

Further possible TRPV2 activators are the endocannabinoid 2-arachidonoyl-glycerol (2-AG) and the chemically related *N*-acyl amino acids (NAAs) *N*-acyl proline and *N*-acyl tyrosine (Qin et al., 2008; De Petrocellis et al., 2011; Raboune et al., 2014; Muller et al., 2018). The presence of anandamide and 2-AG, the main endogenous ligands of the endocannabinoid system (ECS), have been demonstrated for the female reproductive tract, including tubes, uterus, and ovary (follicular fluid), of several species (Schuel et al., 2002; El-Talatini et al., 2009; Maccarrone, 2009; Walker et al., 2019; Fuchs Weizman et al., 2021). Hence, endocannabinoids might act via TRPV2, a possibility that now also remains to be further studied.

Of note, like in the case of the exogenous phytocannabinoid, CBD, used as an activator of TRPV2, the exogeneous cannabinoid

Δ^9-tetrahydrocannabinol (Δ^9-THC), also acts agonistically on TRPV2. Already 40 years ago, it was demonstrated to interfere with rat GC function leading to lower estrogen and progesterone production (Adashi *et al.*, 1983). To our knowledge, details of its modes of action are not well known. Given the presence of TRPV2 in human GCs *in situ* and *in vitro*, GCs and the other TRPV2-expressing ovarian cells are potential targets for THCs. This point is of relevance, considering the use of cannabis and marihuana products, and remains to be examined in depth in future studies.

Taken together, the observations described in our study link the mysterious cation channel TRPV2 to inflammatory processes in the ovary.

Limitations

At present time, in-depth studies in human ovary, including verification of channel-specific actions, are hampered by the lack of exclusively TRPV2-specific pharmacological compounds and the limited experimental possibilities, which are mainly associated with primary human GCs. Other TRPV2-expressing human ovarian cells are not readily accessible.

In GCs, further roles, physiological activators (pressure, endocannabinoid system, growth factors) and modulators (ROS originating from respiration, steroidogenesis, or e.g. NOX pathways) remain to be studied. While physiological inflammatory events are considered essential parts of reproductive events (Yang *et al.*, 2020; Velez *et al.*, 2021), chronic inflammation may be important in reproductive dysfunction. Hence, the involvement of TRPV2 in ovarian diseases, especially where inflammation is reportedly involved, such as in PCOS (Adams *et al.*, 2016), or medical conditions with a known impact on ovarian function, like obesity and aging (Babayev and Duncan, 2022), now await scientific examination.

Supplementary data

Supplementary data are available at *Molecular Human Reproduction* online.

Data availability

The mass spectrometry proteomics data underlying this article have been deposited to the ProteomeXchange Consortium via the PRIDE partner repository (https://www.proteomexchange.org/) with the dataset identifier: PXD041060.

Acknowledgements

We sincerely thank all former lab members who participated directly or indirectly in this study with experimental and technical support. Konstantin Bagnjuk, Sarah Beschta, Jan Blohberger, Theresa Buck, Kim-Gwendolyn Dietrich, Carsten Theo Hack, Lars Kunz, Annette Müller-Taubenberger, and Lena Walenta are gratefully acknowledged.

Authors' roles

K.E. performed the majority of the experiments and performed the corresponding follow-up analysis. K.M.C. performed the mass spectrometry and analyzed the results. C.H., N.K., and A.T. contributed with immunohistochemistry and general technical assistance and support. U.B. and D.B. granted access to human follicular fluids and thus human GCs. G.A.D. provided rhesus tissue and, together with T.F. and A.M. provided conceptional input. A.M. conceived of the study and, together with K.E., designed and supervised the study, and drafted the manuscript. All authors contributed to the final version of the article and approved it.

Funding

This study was funded by a grant from Deutsche Forschungsgemeinschaft (DFG) MA 108031/1, FR 3411/5-1, project 456828204. The Rhesus monkeys were supported in part by the National Institutes of Health (Bethesda, MD; grant no. P51OD011092) to the Oregon National Primate Research Center, Beaverton, Oregon, USA.

Conflict of interest

The authors declare that there are no conflicts of interest regarding authorship or publication of this study.

References

Adams J, Liu Z, Ren YA, Wun WS, Zhou W, Kenigsberg S, Librach C, Valdes C, Gibbons W, Richards J. Enhanced inflammatory transcriptome in the granulosa cells of women with polycystic ovarian syndrome. *J Clin Endocrinol Metab* 2016;**101**:3459–3468.

Adashi EY, Jones PB, Hsueh AJ. Direct antigonadal activity of cannabinoids: suppression of rat granulosa cell functions. *Am J Physiol* 1983;**244**:E177–185.

Agoston A, Kunz L, Krieger A, Mayerhofer A. Two types of calcium channels in human ovarian endocrine cells: involvement in steroidogenesis. *J Clin Endocrinol Metab* 2004;**89**:4503–4512.

Alexandrova E, Pecoraro G, Sellitto A, Melone V, Ferravante C, Rocco T, Guacci A, Giurato G, Nassa G, Rizzo F *et al.* An overview of cadidate therapeutic target genes in ovarian cancer. *Cancers (Basel)* 2020;**12**:1470.

Arici A, Oral E, Bukulmez O, Buradagunta S, Engin O, Olive DL. Interleukin-8 expression and modulation in human preovulatory follicles and ovarian cells. *Endocrinology* 1996;**137**:3762–3769.

Arici A, Oral E, Bukulmez O, Buradagunta S, Bahtiyar O, Jones EE. Monocyte chemo-tactic protein-1 expression in human preovulatory follicles and ovarian cells. *J Reprod Immunol* 1997;**32**:201–219.

Asdell SA. The mechanism of ovulation. *The Ovary* 1962;**1**:435–449.

Ávila J, González-Fernández R, Rotoli D, Hernández J, Palumbo A. Oxidative stress in granulosa-lutein cells from in vitro fertilization patients. *Reprod Sci* 2016;**23**:1656–1661.

Babayev E, Duncan FE. Age-associated changes in cumulus cells and follicular fluid: the local oocyte microenvironment as a determinant of gamete quality. *Biol Reprod* 2022;**106**:351–365.

Bagnjuk K, Mayerhofer A. Human luteinized granulosa cells—a cellular model for the human corpus luteum. *Front Endocrinol (Lausanne)* 2019;**10**:452.

Bagnjuk K, Stöckl JB, Fröhlich T, Arnold GJ, Behr R, Berg U, Berg D, Kunz L, Bishop C, Xu J *et al.* Necroptosis in primate luteolysis: a role for ceramide. *Cell Death Discov* 2019;**5**:67.

Beschta S, Eubler K, Bohne N, Forne I, Berg D, Berg U, Mayerhofer A. A rapid and robust method for the cryopreservation of human granulosa cells. *Histochem Cell Biol* 2021;**156**:509–517.

Biswas A, Ng BH, Prabhakaran VS, Chan CJ. Squeezing the eggs to grow: the mechano-biology of mammalian folliculogenesis. *Front Cell Dev Biol* 2022;**10**:1038107.

Blighe KRS, Lewis M. Publication-ready volcano plots with enhanced colouring and labeling. *Github* 2022. https://github.com/kevinblighe/EnhancedVolcano (8 March 2023, date last accessed).

Blohberger J, Kunz L, Einwang D, Berg U, Berg D, Ojeda SR, Dissen GA, Fröhlich T, Arnold GJ, Soreq H *et al.* Readthrough acetylcholinesterase (AChE-R) and regulated necrosis: pharmacological targets for the regulation of ovarian functions? *Cell Death Dis* 2015;**6**: e1685.

Bogan RL, Murphy MJ, Stouffer RL, Hennebold JD. Systematic determination of differential gene expression in the primate corpus luteum during the luteal phase of the menstrual cycle. *Mol Endocrinol* 2008;**22**:1260–1273.

Boots CE, Jungheim ES. Inflammation and human ovarian follicular dynamics. *Semin Reprod Med* 2015;**33**:270–275.

Botella H, Peyron P, Levillain F, Poincloux R, Poquet Y, Brandli I, Wang C, Tailleux L, Tilleul S, Charrière GM *et al.* Mycobacterial p(1)-type ATPases mediate resistance to zinc poisoning in human macrophages. *Cell Host Microbe* 2011;**10**:248–259.

Brännström M, Norman RJ. Involvement of leukocytes and cytokines in the ovulatory process and corpus luteum function. *Hum Reprod* 1993;**8**:1762–1775.

Buck T, Hack CT, Berg D, Berg U, Kunz L, Mayerhofer A. The NADPH oxidase 4 is a major source of hydrogen peroxide in human granulosa-lutein and granulosa tumor cells. *Sci Rep* 2019;**9**:3585.

Büscher U, Chen FC, Kentenich H, Schmiady H. Cytokines in the follicular fluid of stimulated and non-stimulated human ovaries; is ovulation a suppressed inflammatory reaction? *Hum Reprod* 1999; **14**:162–166.

Buyalos RP, Watson JM, Martinez-Maza O. Detection of interleukin-6 in human follicular fluid. *Fertil Steril* 1992;**57**:1230–1234.

Caterina MJ, Rosen TA, Tominaga M, Brake AJ, Julius D. A capsaicin-receptor homologue with a high threshold for noxious heat. *Nature* 1999;**398**:436–441.

Chai H, Cheng X, Zhou B, Zhao L, Lin X, Huang D, Lu W, Lv H, Tang F, Zhang Q *et al.* Structure-based discovery of a subtype-selective inhibitor targeting a transient receptor potential vanilloid channel. *J Med Chem* 2019;**62**:1373–1384.

Dahm-Kahler P, Ghahremani M, Lind AK, Sundfeldt K, Brännström M. Monocyte chemo-tactic protein-1 (MCP-1), its receptor, and macrophages in the perifollicular stroma during the human ovulatory process. *Fertil Steril* 2009;**91**:231–239.

Dai H, Wang L, Li L, Huang Z, Ye L. Metallothionein 1: a new spotlight on inflammatory diseases. *Front Immunol* 2021;**12**:739918.

De SK, McMaster MT, Andrews GK. Endotoxin induction of murine metallothionein gene expression. *J Biol Chem* 1990;**265**: 15267–15274.

De Petrocellis L, Ligresti A, Moriello AS, Allarà M, Bisogno T, Petrosino S, Stott CG, Di Marzo V. Effect of cannabinoids and cannabinoid-enriched Cannabis extracts in TRP channels and endocannabinoid metabolic enzymes. *Br J Pharmacol* 2011;**163**: 1479–1494.

Duffy DM, Ko C, Jo M, Brännström M, Curry TE. Ovulation: parallels with inflammatory processes. *Endocr Rev* 2019;**40**:369–416.

Elbaz M, Ahirwar D, Xiaoli Z, Zhou X, Lustberg M, Nasser MW, Shilo K, Ganju RK. TRPV2 is a novel biomarker and therapeutic target in triple negative breast cancer. *Oncotarget* 2018;**9**:33459–33470.

El-Talatini MR, Taylor AH, Elson JC, Brown L, Davidson AC, Konje JC. Localisation and function of the endocannabinoid system in the human ovary. *PLoS One* 2009;**4**:e4579.

Espey LL. Ovulation as an inflammatory reaction—a hypothesis. *Biol Reprod* 1980;**22**:73–106.

Espey LL. Current status of the hypothesis that mammalian ovulation is comparable to an inflammatory reaction. *Biol Reprod* 1994; **50**:233–238.

Espey LL, Ujioka T, Okamura H, Richards JS. Metallothionein-1 messenger RNA transcription in steroid-secreting cells of the rat ovary during the periovulatory period. *Biol Reprod* 2003;**68**: 1895–1902.

Eubler K, Herrmann C, Tiefenbacher A, Köhn FM, Schwarzer JU, Kunz L, Mayerhofer A. Ca^{2+} signaling and IL-8 secretion in human testicular peritubular cells involve the cation channel TRPV2. *Int J Mol Sci* 2018;**19**:2829.

Eubler K, Rantakari P, Gerke H, Herrmann C, Missel A, Schmid N, Walenta L, Lahiri S, Imhof A, Strauss L *et al.* Exploring the ion channel TRPV2 and testicular macrophages in mouse testis. *Int J Mol Sci* 2021;**22**:4727.

Field SL, Dasgupta T, Cummings M, Orsi NM. Cytokines in ovarian folliculogenesis, oocyte maturation and luteinisation. *Mol Reprod Dev* 2014;**81**:284–314.

Fiorentino G, Cimadomo D, Innocenti F, Soscia D, Vaiarelli A, Ubaldi FM, Gennarelli G, Garagna S, Rienzi L, Zuccotti M. Biomechanical forces and signals operating in the ovary during folliculogenesis and their dysregulation: implications for fertility. *Hum Reprod Update* 2023;**29**:1–23.

Fuchs Weizman N, Wyse BA, Szaraz P, Defer M, Jahangiri S, Librach CL. Cannabis alters epigenetic integrity and endocannabinoid signalling in the human follicular niche. *Hum Reprod* 2021;**36**: 1922–1931.

Ibeas Bih C, Chen T, Nunn AV, Bazelot M, Dallas M, Whalley BJ. Molecular targets of cannabidiol in neurological disorders. *Neurotherapeutics* 2015;**12**:699–730.

Kanzaki M, Zhang YQ, Mashima H, Li L, Shibata H, Kojima I. Translocation of a calcium-permeable cation channel induced by insulin-like growth factor-I. *Nat Cell Biol* 1999;**1**:165–170.

Kato S, Shiozaki A, Kudou M, Shimizu H, Kosuga T, Ohashi T, Arita T, Konishi H, Komatsu S, Kubota T *et al.* TRPV2 promotes cell migration and invasion in gastric cancer via the transforming growth factor-β signaling pathway. *Ann Surg Oncol* 2022;**29**:2944–2956.

Kawano Y, Zeineh K, Furukawa Y, Utsunomiya Y, Okamoto M, Narahara H. The effects of epidermal growth factor and transforming growth factor-alpha on secretion of interleukin-8 and growth-regulated oncogene-alpha in human granulosa-lutein cells. *Gynecol Obstet Invest* 2012;**73**:189–194.

Kojima I, Nagasawa M. TRPV2. *Handb Exp Pharmacol* 2014;**222**: 247–272.

Landucci E, Pellegrini-Giampietro DE, Gianoncelli A, Ribaudo G. Cannabidiol preferentially binds TRPV2: a novel mechanism of action. *Neural Regen Res* 2022;**17**:2693–2694.

Link TM, Park U, Vonakis BM, Raben DM, Soloski MJ, Caterina MJ. TRPV2 plays a pivotal role in macrophage particle binding and phagocytosis. *Nat Immunol* 2010;**11**:232–239.

Loret de Mola JR, Flores JP, Baumgardner GP, Goldfarb JM, Gindlesperger V, Friedlander MA. Elevated interleukin-6 levels in the ovarian hyperstimulation syndrome: ovarian immunohistochemical localization of interleukin-6 signal. *Obstet Gynecol* 1996; **87**:581–587.

Maccarrone M. Endocannabinoids: friends and foes of reproduction. *Prog Lipid Res* 2009;**48**:344–354.

Machelon V, Emilie D, Lefevre A, Nome F, Durand-Gasselin I, Testart J. Interleukin-6 biosynthesis in human preovulatory follicles: some of its potential roles at ovulation. *J Clin Endocrinol Metab* 1994;**79**:633–642.

Machelon V, Nome F, Duran-Gasselin I, Emilie D. Macrophage and granulosa interleukin-1 β mRNA in human ovulatory follicles. *Hum Reprod* 1995;**10**:2198–2203.

Matousek M, Carati C, Gannon B, Brännström M. Novel method for intrafollicular pressure measurements in the rat ovary: increased intrafollicular pressure after hCG stimulation. *Reproduction* 2001; **121**:307–314.

Molka B, Gwladys B, Dorian B, Lucie M, Mustapha B, Rosalie C, Brigitte G, Hafida KC, Moncef B. Follicular fluid growth factors and interleukin profiling as potential predictors of IVF outcomes. *Front Physiol* 2022;**13**:859790.

Monet M, Gkika D, Lehen'kyi V, Pourtier A, Vanden Abeele F, Bidaux G, Juvin V, Rassendren F, Humez S, Prevarsakaya N. Lysophospholipids stimulate prostate cancer cell migration via TRPV2 channel activation. *Biochim Biophys Acta* 2009;**1793**: 528–539.

Monet M, Lehen'kyi V, Gackiere F, Firlej V, Vandenberghe M, Roudbaraki M, Gkika D, Pourtier A, Bidaux G, Slomianny C *et al.* Role of cationic channel TRPV2 in promoting prostate cancer migration and progression to androgen resistance. *Cancer Res* 2010; **70**:1225–1235.

Muller C, Morales P, Reggio PH. Cannabinoid ligands targeting TRP channels. *Front Mol Neurosci* 2018;**11**:487.

Murayama C, Kaji A, Miyauchi K, Matsui M, Miyamoto A, Shimizu T. Effect of VEGF (vascular endothelial growth factor) on expression of IL-8 (interleukin-8), IL-1beta and their receptors in bovine theca cells. *Cell Biol Int* 2010;**34**:531–536.

Nagasawa M, Nakagawa Y, Tanaka S, Kojima I. Chemotactic peptide fMetLeuPhe induces translocation of the TRPV2 channel in macrophages. *J Cell Physiol* 2007;**210**:692–702.

Neeper MP, Liu Y, Hutchinson TL, Wang Y, Flores CM, Qin N. Activation properties of heterologously expressed mammalian TRPV2: evidence for species dependence. *J Biol Chem* 2007;**282**: 15894–15902.

Oda M, Fujiwara Y, Ishizaki Y, Shibasaki K. Oxidation sensitizes TRPV2 to chemical and heat stimuli, but not mechanical stimulation. *Biochem Biophys Rep* 2021;**28**:101173.

Ortega MS, Wohlgemuth S, Tribulo P, Siqueira LG, Cole JB, Hansen PJ. A single nucleotide polymorphism in COQ9 affects mitochondrial and ovarian function and fertility in Holstein cows. *Biol Reprod* 2017;**96**:652–663.

Perálvarez-Marín A, Doñate-Macian P, Gaudet R. What do we know about the transient receptor potential vanilloid 2 (TRPV2) ion channel? *FEBS J* 2013;**280**:5471–5487.

Perez-Riverol Y, Bai J, Bandla C, García-Seisdedos D, Hewapathirana S, Kamatchinathan S, Kundu DJ, Prakash A, Frericks-Zipper A, Eisenacher M *et al.* The PRIDE database resources in 2022: a hub for mass spectrometry-based proteomics evidences. *Nucleic Acids Res* 2022;**50**:D543–D552.

Pfaffl MW. A new mathematical model for relative quantification in real-time RT-PCR. *Nucleic Acids Res* 2001;**29**:e45.

Piccinni MP, Vicenti R, Logiodice F, Fabbri R, Kullolli O, Pallecchi M, Paradisi R, Danza G, Macciocca M, Lombardelli L *et al.* Description of the follicular fluid cytokine and hormone profiles in human physiological natural cycles. *J Clin Endocrinol Metab* 2021;**106**: e721–e738.

Prasad S, Tiwari M, Pandey AN, Shrivastav TG, Chaube SK. Impact of stress on oocyte quality and reproductive outcome. *J Biomed Sci* 2016;**23**:36.

Pumroy RA, Samanta A, Liu Y, Hughes TE, Zhao S, Yudin Y, Rohacs T, Han S, Moiseenkova-Bell VY. Molecular mechanism of TRPV2 channel modulation by cannabidiol. *eLife* 2019;**8**:e48792.

Qi L, Liu B, Chen X, Liu Q, Li W, Lv B, Xu X, Wang L, Zeng Q, Xue J *et al.* Single-cell transcriptomic analysis reveals mitochondrial dynamics in oocytes of patients with polycystic ovary syndrome. *Front Genet* 2020;**11**:396.

Qin N, Neeper MP, Liu Y, Hutchinson TL, Lubin ML, Flores CM. TRPV2 is activated by cannabidiol and mediates CGRP release in cultured rat dorsal root ganglion neurons. *J Neurosci* 2008;**28**: 6231–6238.

Raboune S, Stuart JM, Leishman E, Takacs SM, Rhodes B, Basnet A, Jameyfield E, McHugh D, Widlanski T, Bradshaw HB. Novel endogenous N-acyl amides activate TRPV1-4 receptors, BV-2 microglia, and are regulated in brain in an acute model of inflammation. *Front Cell Neurosci* 2014;**8**:195.

Richards JS, Liu Z, Shimada M. Immune-like mechanisms in ovulation. *Trends Endocrinol Metab* 2008;**19**:191–196.

Ross HR, Napier I, Connor M. Inhibition of recombinant human T-type calcium channels by Delta9-tetrahydrocannabinol and cannabidiol. *J Biol Chem* 2008;**283**:16124–16134.

Runesson E, Boström EK, Janson PO, Brännström M. The human preovulatory follicle is a source of the chemotactic cytokine interleukin-8. *Mol Hum Reprod* 1996;**2**:245–250.

Santoni G, Amantini C, Maggi F, Marinelli O, Santoni M, Nabissi M, Morelli MB. The TRPV2 cation channels: from urothelial cancer invasiveness to glioblastoma multiforme interactome signature. *Lab Invest* 2020;**100**:186–198.

Santoni G, Farfariello V, Liberati S, Morelli MB, Nabissi M, Santoni M, Amantini C. The role of transient receptor potential vanilloid type-2 ion channels in innate and adaptive immune responses. *Front Immunol* 2013;**4**:34.

Schuel H, Burkman LJ, Lippes J, Crickard K, Forester E, Piomelli D, Giuffrida A. N-Acylethanolamines in human reproductive fluids. *Chem Phys Lipids* 2002;**121**:211–227.

Shibasaki K. Physiological significance of TRPV2 as a mechanosensor, thermosensor and lipid sensor. *J Physiol Sci* 2016;**66**:359–365.

Shibasaki K, Murayama N, Ono K, Ishizaki Y, Tominaga M. TRPV2 enhances axon outgrowth through its activation by membrane stretch in developing sensory and motor neurons. *J Neurosci* 2010; **30**:4601–4612.

Siveen KS, Nizamuddin PB, Uddin S, Al-Thani M, Frenneaux MP, Janahi IA, Steinhoff M, Azizi F. TRPV2: a cancer biomarker and potential therapeutic target. *Dis Markers* 2020;**2020**:8892312.

Sun C, Yang X, Wang T, Cheng M, Han Y. Ovarian biomechanics: from health to disease. *Front Oncol* 2021;**11**:744257.

Sung Y, Yoon I, Han JM, Kim S. Functional and pathologic association of aminoacyl-tRNA synthetases with cancer. *Exp Mol Med* 2022; **54**:553–566.

Trau HA, Brännström M, Curry TE Jr, Duffy DM. Prostaglandin E2 and vascular endothelial growth factor A mediate angiogenesis of human ovarian follicular endothelial cells. *Hum Reprod* 2016; **31**:436–444.

Tyanova S, Temu T, Sinitcyn P, Carlson A, Hein MY, Geiger T, Mann M, Cox J. The Perseus computational platform for comprehensive analysis of (prote)omics data. *Nat Methods* 2016;**13**:731–740.

Velez LM, Seldin M, Motta AB. Inflammation and reproductive function in women with polycystic ovary syndrome. *Biol Reprod* 2021; **104**:1205–1217.

Walker OS, Holloway AC, Raha S. The role of the endocannabinoid system in female reproductive tissues. *J Ovarian Res* 2019;**12**:3.

Wang L, Li Z, Sievert D, Smith DEC, Mendes MI, Chen DY, Stanley V, Ghosh S, Wang Y, Kara M *et al.* Loss of NARS1 impairs progenitor proliferation in cortical brain organoids and leads to microcephaly. *Nat Commun* 2020;**11**:4038.

Wang LJ, Brännström M, Robertson SA, Norman RJ. Tumor necrosis factor alpha in the human ovary: presence in follicular fluid and effects on cell proliferation and prostaglandin production. *Fertil Steril* 1992;**58**:934–940.

Yamashiro K, Sasano T, Tojo K, Namekata I, Kurokawa J, Sawada N, Suganami T, Kamei Y, Tanaka H, Tajima N *et al.* Role of transient receptor potential vanilloid 2 in LPS-induced cytokine production in macrophages. *Biochem Biophys Res Commun* 2010; **398**:284–289.

Yang Z, Tang Z, Cao X, Xie Q, Hu C, Zhong Z, Tan J, Zheng Y. Controlling chronic low-grade inflammation to improve follicle development and survival. *Am J Reprod Immunol* 2020;**84**: e13265.

Zhang D, Spielmann A, Wang L, Ding G, Huang F, Gu Q, Schwarz W. Mast-cell degranulation induced by physical stimuli involves the activation of transient-receptor-potential channel TRPV2. *Physiol Res* 2012;**61**:113–124.

Zhang Y, Yan Z, Qin Q, Nisenblat V, Chang HM, Yu Y, Wang T, Lu C, Yang M, Yang S *et al.* Transcriptome landscape of human folliculogenesis reveals oocyte and granulosa cell interactions. *Mol Cell* 2018;**72**:1021–1034.e4.